NASA Contractor Report 187220

Structural Characterization of High Temperature Composites

J.F. Mandell and D.H. Grande
Massachusetts Institute of Technology
Cambridge, Massachusetts

October 1991

Prepared for
Lewis Research Center
Under Grant NSG3-377

NASA
National Aeronautics and
Space Administration

TABLE OF CONTENTS

	Page
FOREWARD	ii
ABSTRACT	iii
INTRODUCTION	1
LOW TEMPERATURE TEST METHODS	2
HIGH TEMPERATURE TESTING	6
MATERIALS AND APPARATUS	9
TENSILE TEST METHOD	11
TEST RESULTS AND DISCUSSION	15
Nicalon/1723 Glass	15
Nicalon/BMAS Glass-Ceramic	19
0/90 Laminate Tests	22
CONCLUSIONS	24
ACKNOWLEDGEMENTS	24
REFERENCES	25
TABLES	
FIGURES	

FOREWORD

This is the final report for NASA Grant NSG-377 for the period 12/10/82 - 9/30/85. The general objectives of this grant were: (1) to develop mechanical test methods for composite materials for temperatures up to 1000°C; (2) to determine the mechanical properties of available composites up to 1000°C or to their maximum use temperature; (3) to study modes of failure; and (4) to correlate data with theoretical models. Dr. J.F. Mandell was the Principal Investigator on the grant; other major participants were graduate student research assistants D.H. Grande, B.D. Edwards, and J. Jacobs. The NASA-LeRC Project Manager was Dr. C.C. Chamis.

ABSTRACT

Glass, ceramic, and carbon matrix composite materials have emerged in recent years with potential properties and temperature resistance which make them attractive for high temperature applications such as gas turbine engines. At the outset of this study, only flexural tests were available to evaluate brittle matrix composites at temperatures in the 600 to 1000°C range. This report describes the results of an ongoing effort to develop appropriate tensile, compression and shear test methods for high temperature use. A tensile test for unidirectional composites has been developed and used to evaluate the properties and behavior of ceramic fiber reinforced glass and glass-ceramic matrix composites in air at temperatures up to 1000°C. The results indicate generally efficient fiber reinforcement and tolerance to matrix cracking similar to polymer matrix composites. Limiting properties in these materials may be an inherently very low transverse strain to failure, and high temperature embrittlement due to fiber/matrix interface oxidation.

INTRODUCTION

Fiber composites with brittle matrices including glass, ceramic, and carbon have potential properties which may make them attractive structural materials for very high temperature applications. Recent progress in materials and processing research and development has advanced several systems to a stage appropriate for detailed structural evaluation. Composites used in this study were fabricated in a typical process with unidirectional tapes stacked in the desired ply configuration and compression molded at a temperature where the glass matrix would flow sufficiently to form fully densified material [1]. Most fibers can be degraded to some extent at very high processing temperatures, and an effective technique for developing high temperature resistance is to use glass matrices which can be compression molded at relatively low temperatures, followed by a crystallization step to form a glass-ceramic matrix. A variety of glass and glass-ceramic matrices have been successfully fabricated with several carbon and ceramic fibers [1-3].

The mechanical properties of these materials have been evaluated in most studies by three and four point flexural specimens, which are convenient to run on small samples of material and at elevated temperatures. While a number of programs are underway to develop high temperature tests, only a few studies have reported high temperature properties other

than flexure [4-6]. Flexural tests of sufficient span to depth ratio usually produce a tension dominated failure mode with qualitative strength and damage trends which agree with tensile data. However, as with other fiber composites, flexural tests do not give adequate material property data for quantitative structural characterization [4-7]. Figure 1 shows the significant difference in flexural and tensile stress-strain curves for specimens taken from a single plate of one of the materials used in this study (the strain in both tests was determined with strain gages). This particular batch of material showed much less than optimum properties as discussed later, but failure was tension dominated in both tests, and both tests would show an increase in ultimate strength of a factor of two or more for a more optimized material. The only property which is quantitatively similar in flexure and tension in Figure 1 is the initial modulus. A full range of tensile, compressive, and shear properties are required to meaningfully evaluate composites for high temperature applications.

LOW TEMPERATURE TEST METHODS

To obtain acceptable properties in various (planar) directions, advanced fiber composites with polymeric matrices are usually fabricated as laminate structures composed of individual unidirectional plies oriented in selected directions to give the desired balance of properties for

particular applications. The behavior of the composite is rationalized by a set of properties for each (usually identical) ply combined with a suitable analysis to predict laminate behavior from the ply properties [8]. The minimum ply properties required for laminate design and analysis are the longitudinal and transverse tensile and compressive moduli and strengths, Poisson's ratios, and the in-plane shear modulus and strength. Thermomechanical analysis of laminates is also commonly required, so that the coefficients of thermal expansion in the longitudinal and transverse directions are included as ply properties, both for prediction of the laminate expansion coefficients in various directions and the calculation of thermal residual stresses within each ply of the laminate. Thermal residual stresses are often a significant fraction of the polymer composite ply transverse strength, particularly for high processing temperature systems.

The extreme strength anisotropy and planar (sheet) form of most unidirectional fiber composites have complicated the development of appropriate test methods for the required ply properties. Dumbbell-shaped specimens are often used for tensile properties of polymers and multidirectional composites [9], but unidirectional longitudinal composites split parallel to the fibers at the specimen shoulder, shifting the failure to within the grip area where the complex stress state renders the results invalid. The

dumbbell shape can often be used for transverse tensile properties. Most ply properties for advanced polymer matrix composites are now obtained with straight-sided strips of material to which tapered end tabs are bonded with a suitable adhesive; typical test methods are described in Refs. 10 and 11. Gage-section tensile failures can be obtained in this manner with most unidirectional composites.

Compression tests present greater problems due to the variety of possible failure modes [12], which include elastic specimen buckling, successive delamination and buckling of surface plies, end brooming and axial splitting, as well as what might be termed material compressive failurs which may involve microscale modes of shear, fiber buckling, or fiber failure. The mode of failure often changes when the specimen size or test method is changed, as from compressive end loading to shear loading through tabs, and depending on whether constraint against buckling is applied along the gage section [11]. Analogous mode and strength variations may be expected in applications, depending on geometry, buckling constraint and load introduction. Thus, a single compression strength value may have little general meaning in composites. Currently, the most important compression tests [11] for establishing ply properties in polymer composites introduce the load through shear using bonded tabs much like tabbed tensile coupons; lateral buckling constraint is usually provided.

In-plane unidirectional shear properties and interlaminar shear properties are also difficult to determine, and a number of test methods are available [11,13]. Since most composites are not readily available as rods or tubes, direct torsion tests are usually not practical. Other tests, whether off-axis tension, rail shear or Iosepescu [13] provide reliable values of shear modulus, but differing levels of uncertainty for the complete shear stress-strain curve to failure, which is usually nonlinear.

The shear strength for unidirectional material and laminates is frequently determined with the short beam shear test [11]; when failure is in the proper mode, this test gives results useful for materials development and for comparisons between materials, but not for design.

Other test methods such as three- and four-point flexure [11], impact [14], and fracture toughness [15] are also used with polymer matrix composites, but not for the purpose of obtaining basic data for design and analysis. Fracture toughness in particular has not been a generally useful test method or property for continuous fiber polymer matrix composites. Many composites are not notch sensitive even for notches of one cm or more in length; of those that are notch sensitive, some of the more brittle may be analyzed using linear elastic fracture mechanics for certain stress directions and ply arrangements [15]. However, the fracture toughness and degree of notch sensitivity are not a simple consequence of unidirectional ply properties, but depend

primarily on the details of ply configuration (orientation of different plies and ply stacking sequence) for each particular laminate. In most cases the notch sensitivity for catastrophic failure is a consequence of the extent of the stable matrix/interface cracking (damage zone) which forms in areas of high stress concentration; the larger the stable cracking damage zone, the lower the overall notch sensitivity [15]. Since failure in most applications of composites does not occur by a single dominant crack, fracture mechanics has not been of great interest even though it may be applicable for certain narrow ranges of structure. Localized cracks parallel to the fibers of individual plies, and delaminations between plies are limited areas where fracture mechanics has been of greater interest [16].

HIGH TEMPERATURE TESTING

A number of factors combine to cause difficulties with high temperature testing of continuous fiber reinforced composites, paricularly those with brittle glass and ceramic matrices:

(1) Flexural test data are much less useful than with monolithic glasses and ceramics.

(2) Load introduction in unidirectional tensile and compressive tests is difficult due to the low

transverse and shear properties associated with poor fiber/matrix bonding and brittle, high modulus matrices. For example, serrated grip faces result in fragmentation of the specimen surface as shown in Figure 2.

(3) The unidirectional strength arisotropy is similar to that with polymer matrix composites despite the much higher matrix modulus. As a result, dumbbell-shaped longitudinal specimens have shoulder-splitting problems similar to those with polymer composites.

(4) As with standard polymer composites tests, adhesively bonded tabs function well for load introduction. However, bonded tabs require tough adhesives which are not available for high temperature use.

(5) Most material systems of interest are currently available only in small plates of 10-15 cm length and width at best, which limits load transfer distances.

The consequence of these problems is that the tensile and compressive stress-strain behavior of longitudinal specimens cannot be evaluated at high temperatures using

established test methods, except for initial modulus up to the matrix cracking strain (with flexural tests). Several studies have been conducted [4,5] or are in progress [6,7] to develop suitable high-temperature mechanical tests. While differing materials systems have been used in these studies, the experiences reported are generally consistent. The most challenging test appears to be longitudinal tension, where attempts to use dumbbell-shaped specimens have resulted in severely reduced gage section width and thickness, often in several stages with difficult machining and often without achieving consistent gage-section failures [4-7]. As discussed later, tensile testing with multidirectional laminates using dumbbell specimens has been much less problematical [4,5,7].

Simulated shear tests using $\pm$ 45° or unidirectional off-axis specimens have also been successfull [4], and it appears that interlaminar shear tests based on short beam [5] and double-notched [5,7] specimens function properly at low temperatures and could be used at high temperatures. Compressive tests based on unconstrained short dumbbell-shaped specimens appeared to fail in the gage section and give meangingful results, as reported in Ref. 4.

Instrumentation for high temperature testing is also a potential problem area, particularly at temperatures significantly above 1000°C. Furnaces with air, inert gas, and vacuum conditions which are compatible with various mechanical testing machines are commercially available up to

at least 2000°C. However, the construction of gripping apparatus may be difficult much above 1000°C unless ceramics can be used, as is commonly done in flexural test apparatus. Strain measurement creates problems, as strain gages are not available for temperatures in this range. Optical methods are being considered [7], but the usual method is extensometers which are external to the furnace, contacting the specimen with quartz or ceramic rods [4]. While successful tension tests have been reported up to temperatures of 1100°C [4], it should be recognized that these tests usually require long heat-up and cool-down times, so that a typical test takes several hours to conduct.

MATERIALS AND APPARATUS

The materials used in this study were supplied by Corning Glass Works, as were the properties and information given in Table 1. The BMAS glass/ceramic matrix system was an early experimental batch which gave properties well below those which have since been achieved, as discussed later. Both materials are composed of unidirectional plies of continuous fibers with a fiber content of 35 to 40% by volume, and with little or no porosity. At this fiber content the distribution of fibers is often very uneven, as shown in later micrographs.

An important aspect of this class of brittle, high modulus matrix composites is that efficient reinforcement by

the fibers requires a fiber/matrix interface which will debond as matrix cracks form and propagate. This allows the full fiber strength and failure strain to be realized in the composite even though the matrix may crack at strains in the vicinity of 10-20% of the fiber failure strain. As will be shown later, a very strong bond between fibers and matrix results in brittle behavior, with matrix cracks propagating through the fibers. Thus, to be successful, glass and glass/ceramic composites must be fabricated so as to prevent very high interface strengths. Recent studies [2,3] have shown that under proper processing conditions the materials in Table 1 (and similar materials) form a carbon layer at the interface as a result of favorable diffusion and chemical reactions between the Nicalon fibers and the matrix.

Test specimens were cut from plates with a diamond-edged cutoff wheel, and ground to the desired shape with a 300 grit diamond wheel. Grinding was done with a water soluble lubricant at a rate of material removal of approximately 5-10 m/pass. Holes in the grip section of some multidirectional specimens were drilled with a diamond grinding bit, while divots for extensometer contact were made with a No. 1 center drill to a depth of about 0.2 mm, and an included edge angle of 110°.

The test system used in this program is a servohydraulic testing machine fitted with an Instron Mod. 3117 high temperature furnace system described in Table 2. The system is designed for testing to $1000^{\circ}C$. The tension grips to be

discussed later were adapted from Applied Test Systems Mod. 4053A wedge couplings. All tests were run in air with a heat-up time of 1 to 2 hours and displacement rates which produced failure in several minutes (strain rates on the order of 10^{-4}/s).

TENSILE TEST METHOD

Figures 3-5 illustrate the tensile test method developed in this study for unidirectional materials. The specimen shape has a constant width but a reduced thickness in the gage section produced by wet grinding in small increments. Figure 4 gives the dimensions which were found to yield satisfactory results for 3 to 5 mm thick unidirectional Nicalon/1723 glass and BMAS; the width was a constant 6.4 mm in all cases, and the gage section thickness was .75 to 1.3 mm. The thickness is reduced in two stages, first following a 5^{o} taper, then a 76 mm radius with a smooth transition to the gage section. Smooth metal wedge blocks are fit to the straight and 5^{o} taper sections as shown in Figure 3; the metal used depends on the test temperature.

When a displacement is applied to the grip, load is introduced through the 5^{o} taper section, which is also compressed normal to the surface to suppress splitting at the shoulder. The 76 mm transition outside the wedge blocks insures that failure will not initiate from the stress concentration at the edge of the wedge block. The 76 mm

radius has proven sufficient in most cases to prevent shoulder splitting in this region for the very slight thickness reduction between the wedge blocks and the gage section. The resulting overall specimen length of 76 mm for a 19 mm gage length is short enough for most small samples available in this study. A larger transition radius such as 150 mm is recommended if larger samples are available. Most longitudinal and transverse specimens failed in the gage section as shown in Figures 5 and 6, despite some local shoulder splitting evident in Figure 5. Many failures were close to the end of the machined radius, and some spread into the grips after initiating in the gage section.

The specimen in Figure 4 has also been used for 0/90 ply configurations, but with an increased tendency toward shoulder failures. With multidirectional laminates it is necessary to provide sacrificial plies to be ground away in the gage section, leaving a balanced laminate configuration. For the case tested, a Nicalon/BMAS plate was fabricated with 16 plies in the configuration $[(90/0)_4]_s$. The average ply thickness was 0.325 mm, but the plies have a slight waviness, so that it was difficult to leave a perfectly symmetrical laminate in the gage section. The actual cases as ground were approximately $[(90/0)_2]_s$ with half-thickness 90's on the outside, and $[0/90/0]_s$, as shown in Figure 7. A dumbbell-shaped specimen has been used sucessfully for multidirectional laminates of a similar material [4], and may provide a more practical geometry as discussed later.

One area of difficulty in conducting tensile tests has been with the extensometers. Figure 8 shows the axial extensometer system with detail of the quartz rod contact at the specimen surface. The extensometer rods must be held against the specimen surface divots during thermal expansion as the test system is heated-up for about two hours, and then must follow the specimen translation as well as the strain between the rods during testing. Initial extensometer alignment and seating must be precise. The extensometer slipped completely out of the surface divots in about 20% of the tests; in some other tests there appeared to be slight movement of the rod tips in the divots, leading to a nonlinear response. Figure 9 shows a typical case of nonlinear extensometer response as compared to strain gage output on the same specimen (at room temperature). Despite these problems, in most cases the longitudinal extensometer appeared to behave satisfactorily over the 20 to 1000°C test temperature range.

Considerably more difficulty was encountered with the transverse extensometer, which is designed for use with round specimen cross-sections. When used with the flat specimens to determine Poisson's ratio the response was not reliable, apparently dominated in many cases by slight twisting or misalignment relative to the specimen edges. This problem may be solved in ongoing efforts to modify the tip geometry of the transverse extensometer quartz rods. In principle, the general approach to transverse strain measurement with

this extensometer system should be successful with specimens of this type, but it has not yet received sufficient attention to overcome the current difficulties. The Poisson's ratio data in Table 3 were obtained at room temperature with strain gages.

There are several additional restrictions in using the longitudinal extensometer. The quartz rod tips are brittle, and can be chipped or broken if they are in contact with the specimen at fracture. In many tests the extensometer was removed prior to specimen fracture, with the remainder of the stress-strain curve extrapolated based on the load-stroke curve which was recorded simultaneously (extrapolated data are shown as a dashed line). Room temperature tests also included front and back strain gages in many cases, and these occaisionally showed bending effects in the specimens either from misalignment or nonuniform material distribution. The one-sided extensometer cannot detect these effects, so it is desirable to precheck the specimen at room temperature with strain gages at low loads prior to high temperature testing. The very low strain to initial cracking when off-axis plies are present renders this procedure very difficult if the undamaged stress-strain curve is to be determined at high temperatures. Use of the extensometers can also lead to specimen cracking at the surface divots, but this has been greatly reduced or eliminated by the use of very shallow surface divots described earlier.

TEST RESULTS AND DISCUSSION

Nicalon/1723 Glass

The Nicalon/1723 glass composite shows behavior which is typical of optimized materials in this class, although many details vary from system to system. Figure 10 shows a longitudinal tensile stress-strain curve which includes several unloading cycles. Below 0.1% strain the behavior is linear elastic, with a Young's modulus of 124 GPa, close to the simple rule of mixtures prediction from the matrix and fiber properties. The curve becomes strongly nonlinear beginning around 0.1 to 0.2% strain, then becomes nearly linear again above 0.4 to 0.5%. Failure occurs close to the average fiber failure strain, and at a tensile ultimate strength close to the fiber strength multiplied by the fiber volume fraction, V_f (fibers extracted after fabrication usually show a lower strength than in Table 1 [17]). The elastic modulus at high strains also approaches that of the fibers multiplied by V_f, ignoring the matrix. The mechanical properties for this and the BMAS matrix system are listed in Table 3. Systems with very extensive fiber pullout may also show a tail on the stress-strain curve after the maximum stress [18].

The longitudinal stress-strain behavior in Figure 10 is very close to that of a model brittle matrix system as described by Aveston et al. [19]. The nonlinearity at 0.1 to

0.2% strain corresponds to the onset of matrix cracking, which reaches a saturation density by 0.4 to 0.5% strain; the saturation matrix crack density is on the order of a 0.1mm spacing, as indicated in Figure 11. Figure 11 also shows the fracture surface in profile, with typical fiber pullout lengths of about 10 to 20 fiber diameters. The nonlinearity in Fig. 10 is much greater than for polymer matrix composites because of the much higher ratio of matrix to fiber modulus and the relatively low fiber content.

It is evident that most of the behavior in Fig. 10 is optimum for the given fiber and matrix properties, so that little improvement in the composite could be achieved at this fiber content without improving the fibers or matrix. However, theoretical treatment and some experimental evidence [17-19] suggest that the stress and strain at which matrix cracking develops may be varied. Fracture mechanics treatment of a matrix crack propagating past fibers indicates that the resistance to opening of the matrix crack along the debonded fibers will determine whether matrix cracks can propagate. The resistance to matrix cracking will increase with an increase in debonding or sliding resistance at the interface, an increase in fiber content (more fibers) or a decrease in fiber diameter (more interface area for the same V_f). Table 3 lists the interfacial bond shear strength for the fiber/matrix interface determined by the microdebonding test method illustrated in Figure 12 [20]. Also listed are tentative data for the frictional sliding resistance of the

debonded interface determined in the microdebonding apparatus by compressing the fiber into the matrix at higher forces, following the technique and analysis of Marshall [21]. Of the composite systems which have been tested in this manner to date, the bond strength and interface frictional resistance are relatively high for the Nicalon/1723 system, and so improvement in matrix crack resistance from a higher bond strength or friction may not be practical without risking composite embrittlement. However, neither the limits nor the interpretation of bond strength for these materials are well established. The high interface properties for this material may also reflect thermal residual stresses, as the 1723 glass has a higher coefficient of thermal expansion than does the fiber. The higher bond properties are also evidenced in the fiber pullout length on the fracture surface, which is considerably shorter than reported for systems with a similar failure strain but lower matrix coefficient of expansion, such as Nicalon/LAS [5,18].

The relatively high interface properties should help the composite mechanical properties in off-axis directions. However, the transverse tensile properties given in Table 3 are still very low, and most specimens failed in handling; similar data are reported for other systems [1,22]. The transverse strain to failure in the range of 0.03 to 0.04% is of particular concern, as it is well below the matrix cracking strain in longitudinal specimens. In fact, most transverse unidirectional specimens either fail during

handling or else show negligible strength due to the presence of flaws, so testing and interpretation are difficult. The low transverse strain to failure must be expected for materials in this class due to the effects of fibers creating stress concentrations and flaws not present in the neat matrix or longitudinal direction. A low fiber/matrix bond strength would be expected to exacerbate this problem, and the high interface properties for the Nicalon/1723 should be helpful. However, the interface properties represent shear strengths with a compressive normal component, and their applicability to transverse tension needs further study.

Practical composite materials are usually constructed with plies oriented in several directions, so that some are off-axis relative to an applied uniaxial stress. The low off-axis properties should then produce cracking at low strains in these plies, and the stress-strain curve should become nonlinear at an even lower strain as discussed later. If composites of this type are to function in practical situations, it may be necessary to tolerate some off-axis ply (stable) cracking, particularly in areas of stress concentration. If this is the case, then the interface and fibers must be able to withstand exposure to the environment at such crack sites. As indicated in the next section, current materials which depend on a carbon layer at the interface have a problem in this area at elevated temperatures in oxidizing environments.

Figures 13 and 14 show the effect of temperature (in

air) on the Nicalon/1723 longitudinal tensile strength. The general stress-strain behavior was not significantly affected by temperature up to 500°C, above which the strength decreased. The drop in properties was expected around 600°C based on a softening trend in the matrix modulus. At 600°C some specimens showed a significant increase in fiber pullout on the fracture surface, possibly as a result of release of the residual compression stress at the interface (Fig. 15). Table 4 gives individual test results for the 1723 and BMAS matrix systems at various temperatures.

Nicalon/BMAS Glass-Ceramic

As noted earlier, the batch of Nicalon/BMAS used in this study did not have the best properties achievable with this system. As shown in Figure 16 and Table 4, longitudinal stress-strain curves generally did not get past the nonlinear matrix cracking regime evident for an optimized material in Figure 10, and the failure strain did not approach that of the Nicalon fibers. Comparison of 4-point flexural strength data from these batches with other batches at Corning showed about half of the flexural strength of the best batches (flexural failures were tension dominated). The origin of this problem does not appear to be in the carbon layer at the interface, as the bond strength values in Table 3 are in the expected low range; the frictional sliding resistance is on the same order as that reported for Nicalon/LAS glass-ceramic

by Marshall [21]. Further tests will be run on other batches to clarify the origin of the problem.

Despite the deficiencies of this batch of material, it still allows study of an interesting aspect of behavior found in other high temperature glass-ceramic matrix systems [17]. As the test temperature is increased in the air atmosphere used in all cases, the strength and strain to failure initially increase up to about 650°C, as typical specimens withstand higher levels of matrix cracking without failure. By 800°C the properties have decreased significantly, and a further decrease occurs up to the maximum test temperature of 1000°C. Figure 17 shows the change in longitudinal tensile stength with temperature, while Figure 18 gives the corresponding failure strain data. It should be noted that the heat-up time for the high temperature tests is about two hours, with about 30 minutes at test temperature prior to loading. The loading rate of the test is such that failure occurs in several minutes.

The sharp drop in strength and strain to failure in the 800 to 1000°C range is accompanied by a change in the fracture surface appearance. Below this temperature the usual fiber pullout is found over the entire fracture surface (Figure 19). However, at 1000°C a region of flat, brittle fracture is evident around the exposed edges of the fracture surface, as reported for other similar materials [17]. Figures 19 and 20 show micrographs of the flat fracture region and the interior.

The surface embrittlement effect in similar systems has generally been blamed on oxidation of the interface carbon layer. To explore this question in the present case, a series of experiments have been run with the microdebonding test in Figure 12. One such case is given in Figures 21 and 22. A block of the Nicalon/BMAS with one ground surface and one as-molded surface was conditioned at 1000°C in an air atmosphere with no mechanical load for 12 hours. The specimen was then sectioned and polished as shown in Figure 21; the as-molded surface contained a layer of pure matrix outside of the first fibers, so that the fiber/matrix interfaces were not exposed. Figure 22 gives the fiber/matrix interfacial shear strength across the cross-section shown in Fig. 21; the left scale is the average compressive load applied to the fibers at debond initiation, from which the interfacial shear strength is calculated using a finite element analysis [20]. The interface strength is low from the first fibers at the as-molded surface though the thickness, to within about 0.5mm of the ground surface. The data are close to the value of 46 MPa listed for control material in Table 3. However,as the ground surface is approached in different locations, the bond strength is observed to increase rapidly, with many values exceeding 10 times those on the interior. The data in Figure 22 are plotted together for all locations, while the bond strength rise approaching the ground surface at particular locations occurred at different depths in from the surface, apparently

reflecting the local fiber arrangement.

The results in Figure 22 show that the interface does increase greatly in strength when exposed in air at 1000°C at a ground surface, or when there is an apparent path for oxidation to penetrate along various interfaces into the interior. Near the exposed end of a block where fibers were cut, high bond strengths were observed all across the cross-section, as oxidation tunnelled in from the fiber ends. The tensile specimens used in this study were ground on all surfaces, and further interface exposure is to be expected as matrix cracks form near the knee in the stress-strain curve. It is apparent that the drop in tensile properties at high temperatures was caused by an increase in fiber/matrix bond strength and consequent embrittlement. While matrix layers may protect specimens with as-molded surfaces in the absence of matrix cracking, the carbon layer at the interface in current materials is a major detriment to their application in high temperature oxidizing environments. The embrittlement effect is not observed in similar materials in non-oxidizing atmospheres, and the properties are maintained to well above 1000°C [1].

0/90 Laminate Tests

The test specimen shown in Figure 4 has also been used to test Nicalon/BMAS laminates molded in the ply

configuration $[(90/0)_4]_s$. As discussed earlier (Fig. 7), these specimens were ground in the thickness direction to the desired shape, leaving a symmetrical laminate in the gage section. The ply interfaces were not perfectly planar, so that grinding to leave the desired configuration was difficult. The resulting material did not show a uniform ply thickness for the outermost ply.

Figure 23 gives the 20°C stress-strain curve for specimen 10B in Figure 7. The front and back longitudinal strain gages show differing strains at high stresses, and the same was true of the configuration 10A. While some strain difference may have been due to misalignment and nonsymmetry in the gage section, this high stress response appeared to derive primarily from greater matrix cracking on side 2 than on side 1. The high modulus matrix results in a significant structural nonsymmetry if matrix cracking is not symetrically distributed through the thickness. This apparent effect was also observed with some unidirectional specimens, but to a lesser extent. The 0/90 specimens also tended to fail closer to the specimen shoulder than did unidirectional specimens.

The experience with grinding 0/90 specimens to the shape in Figure 4 suggests that a specimen geometry which would preserve the as-molded thickness is desirable. A width-tapered specimen described in Ref. 4 has given gage-section failures for a variety of ply configurations including 0/90 and $\pm$ 45. The latter configuration would also allow the calculation of a simulated shear stress-strain curve following Ref. 11, and will be pursued in the future.

CONCLUSIONS

High temperature testing of fiber composites requires new test methods and improved strain-measuring capability. A tensile test method developed in this program works well for unidirectional materials, giving gage section failures up to 1000°C and using relatively small material samples. The composite properties can approach theoretical expectations based on fiber and matrix properties and the fiber content. However, the off-axis strain to failure is inherently very low, and surface oxidation embrittlement occurs at high temperatures.

ACKNOWLEDGEMENTS

All materials tested in this program were supplied by Corning Glass Works, while the high temperature testing equipment was donated by Instron Corp. under a cooperative research program. The authors are also grateful for helpful discussions with Dr. K. Chyung at Corning Glass Works and Dr. K. Prewo at United Technologies Research Center.

REFERENCES

1. Prewo, K.M., "Ceramic and Carbon Fiber Reinforced Glasses," Proc. of the Metal and Ceramic Matrix Composite Processing Conf., Battelle Columbus Labs, Columbus, OH (1984).

2. Cooper, R.F. and Chyung, K., "Structure and Chemistry of Fiber-Matrix Interfaces in Nicalon Fiber-Reinforced Glass-Ceramic Composites," presented at American Ceramics Society, 88th Annual Meeting, Chicago (1986).

3. Taylor, M., "Interface Characteristics of Polymer-Derived Fibers in Glass-Ceramic Matrices," presented at American Ceramics Society, 88th Annual Meeting, Chicago (1986).

4. Prewo, K.M., "Advanced Characterization of SiC Fiber Reinforced Glass-Ceramic Matrix Composites," ONR Contract N00014-81-C-0571, Report R83-915939-1, United Technologies Research Center, East Hartford, CT (1983).

5. Prewo, K.M., and Layden, G.K., "Advanced Fabrication and Characterization of SiC Fiber Reinforced Glass-Ceramic Matrix Composites," ONR Contract N00014-81-C-0571, Report R84-916175-1, United Technologies Research Center, East Hartford, CT (1984).

6. Mah, T.-I., "Environmental Effect on Ceramic Matrix Composites at Elevated Temperatures," presented at American Ceramics Society, 88th Annual Meeting, Chicago (1986).

7. Larsen, D.C., Stuchly, S.L., Bortz, S.A., and Ruh, R., in Metal Matrix, Carbon, and Ceramic Matrix Composites 1985, NASA Conf. Pub. 2406, J.D. Buckley, ed., NASA Scientific and Technical Branch, (1985) pp. 313-334.

8. S.W. Tsai and H.T. Hahn, Introduction to Composite Materials, Technomic, Westport, CT (1980).

9. ASTM Test Method D638-82a, Type I (1982).

10. ASTM Test Method D3039-76 (1976).

11. J.M. Whitney, I.M. Daniel and R.B. Pipes, Experimental Mechanics of Fiber Reinforced Composite Materials, The Society for Experimental Stress Analysis, Brookfield Ctr., CT Ch. 4 (1982).

12. H.T. Hahn and J.G. Williams, "Compression Failure Mechanisms in Unidirectional Composites," NASA TM85834, NASA-Langley Research Center (1984).

13. D.E. Walrath and D.F. Adams, "The Iosipescu Shear Test as Applied to Composite Materials," Experimental Mechanics 23, 105 (1983).

14. J.G. Williams and M.D. Rhodes, "Effect of Resin on Impact Damage Tolerance of Graphite/Epoxy Laminates," in Composite Materials, Testing and Design (Sixth Conference) STP 787, I.M. Daniel, ed., ASTM, p. 450 (1982).

15. F.J. McGarry, J.F. Mandell and S.S. Wang, "Fracture of Fiber Reinforced Composites," Polymer Engineering and Science 16, 609 (1976).

16. D.J. Wilkins, J.R. Eisenmann, R.A. Camin, W.S. Margolis and R.A. Benson, "Characterizing Delamination Growth in Graphite/Epoxy," in Damage in Composite Materials, STP 775, K.L. Reifsnider, ed., ASTM, p. 168 (1982).

17. Prewo, K.M., "Fiber Reinforced Glasses and Glass Ceramics," presented at American Ceramics Society, 88th Annual Meeting, Chicago (1986).

18. Marshall, D.B., and Evans, A.G., J. Am. Ceram. Soc., Vol. 68, pp. 225-231 (1985).

19. Aveston, J., Cooper, G.A., and Kelly, A., in Properties of Fibre Composites; Conference Proceedings, National Physical Laboratory, I.P.C. Service and Technology Press, Guildford, pp. 15-26 (1971).

20. Mandell, J.F., Grande, D.H., Tsiang, T.-H., and McGarry, F.J., in Composite Materials: Testing and Design (Seventh Conference), STP 893, J.M. Whitney, ed., ASTM, Phil., pp. 87-108 (1986).

21. Marshall, D.B., Comm. Am. Ceram. Soc., Vol. 67, pp. C259-C260 (1984).

22. Sbaizero, O. and Evans, A.G., J. Am. Ceram. Soc., Vol. 69, pp. 481-486 (1986).

TABLE 1 TYPICAL FIBER AND BULK MATRIX 20°C PROPERTIES

	NICALON® FIBER	1723 GLASS MATRIX	BMAS III GLASS-CERAMIC MATRIX
FIBER DIAMETER (μM)	10-15	----	----
DENSITY (g/CM^3)	2.55[b]	2.64	2.77
COEFF. THERMAL EXP ($10^{-7}/°C$)	31[c]	45.8	17(25-300°C)
YOUNG'S MODULUS (GPa)	193[b]	86	106
TENSILE STRENGTH (GPa)	2.07[b]	----	----
POISSON'S RATIO	----	.24	----
APPARENT MAX. USE TEMP (°C)	1100-1300[c]	600-700	1200-1250
COMPOSITION	SILICON-OXYCARBIDE[d]	ALUMINOSILICATE, (BaO, MgO, CORNING CODE 1723 Al_2O_3, SiO_2)	

[a]Most Data Supplied by K. Chyung, Corning Glass Works Except as Noted.
[b]Ref. 1, [c](Nippon Carbon), [d]Ref. 3.

TABLE 2

DEDICATED HIGH TEMPERATURE COMPOSITES TESTING FACILITY

1. INSTRON MOD. 1331 SERVOHYDRAULIC TESTING MACHINE, 10,000 LB (44KN) CAPACITY

2. INSTRON MOD. 3117 HIGH TEMPERATURE FURNACE SYSTEM (1000^{o} MAX. TEMP, AIR ATMOSPHERE)

   - o SPLIT FURNACE WITH SELF ADAPTIVE MICROPROCESSOR CONTROLLER
   - o WATER COOLED ADAPTERS WITH ALIGNMENT RINGS
   - o REVERSE-STRESS PULLRODS
   - o QUARTZ ROD AXIAL AND TRANSVERSE EXTENSOMETERS

TABLE 3 TYPICAL UNIDIRECTIONAL COMPOSITE PROPERTIES

($20^{\circ}C, V_f = .35\text{-}40$)

	NICALON^{R}/1723	NICALON^{R}/BMAS
LONGITUDINAL TENSILE MODULUS (GPa)	128	144
TRANSVERSE TENSILE MODULUS (GPa)	101	---
POISSON'S RATIO (LT)	.24	.20
LONGITUDINAL TENSILE STRENGTH (MPa)	734	225
TRANSVERSE TENSILE STRENGTH (MPa)	27*	---*
LONGITUDINAL TENSILE FAILURE STRAIN (%)	1.2	.37
TRANSVERSE TENSILE FAILURE STRAIN (%)	.035*	---*
FIBER/MATRIX INTERFACIAL SHEAR STRENGTH (MPa)	185	46
SLIDING FRICTION OF DEBONDED FIBER (MPa)	86	2.8
SHORT BEAM INTERLAMINAR SHEAR STRENGTH (MPa)	73	31

*A Number of Apparently Flawed Specimens With Strength Less Than 5 MPa Are Not Included.

Table 4 Longitudinal Tensile Data

No.	Matrix	Test Temp(^{o}C)	E_L (GPa)	UTS_L (MPa)	Ult. Strain (%)
4A	1723	20	----	714	---
4B	1723	20	124	754	1.3
4C	1723	400	----	688	---
4F	1723	400	127	652	.83
4G	1723	500	----	624	---
4H	1723	500	136	613	.62
4I	1723	500	150	677	1.06
4K	1723	550	121	599	1.0
4D	1723	600	----	471	---
4J	1723	600	----	517	---
4L	1723	600	138	482	.81
8C	BMAS	20	146	223	.24
8D	BMAS	20	148	234	.39
8M	BMAS	20	150	232	.44
8L	BMAS	600	119	252	.53
8N	BMAS	600	132	254	.56
8R	BMAS	650	147	335	---
8V	BMAS	800	124	168	.44
8O	BMAS	800	----	127	

Table 4 (Cont.)

No.	Matrix	Test Temp(°C)	E_l (GPa)	UTS_L (MPa)	Ult. Strain(%)
8W	BMAS	800	132	177	.20
8B	BMAS	900	----	109	---
8A	BMAS	1000	----	154	---
8E	BMAS	1000	----	99.9	---
8Q	BMAS	1000	134	146	.15
8S	BMAS	1000	150	141	.085
8T	BMAS	1000	125	132	.105
8U	BMAS	1000	----	106	---

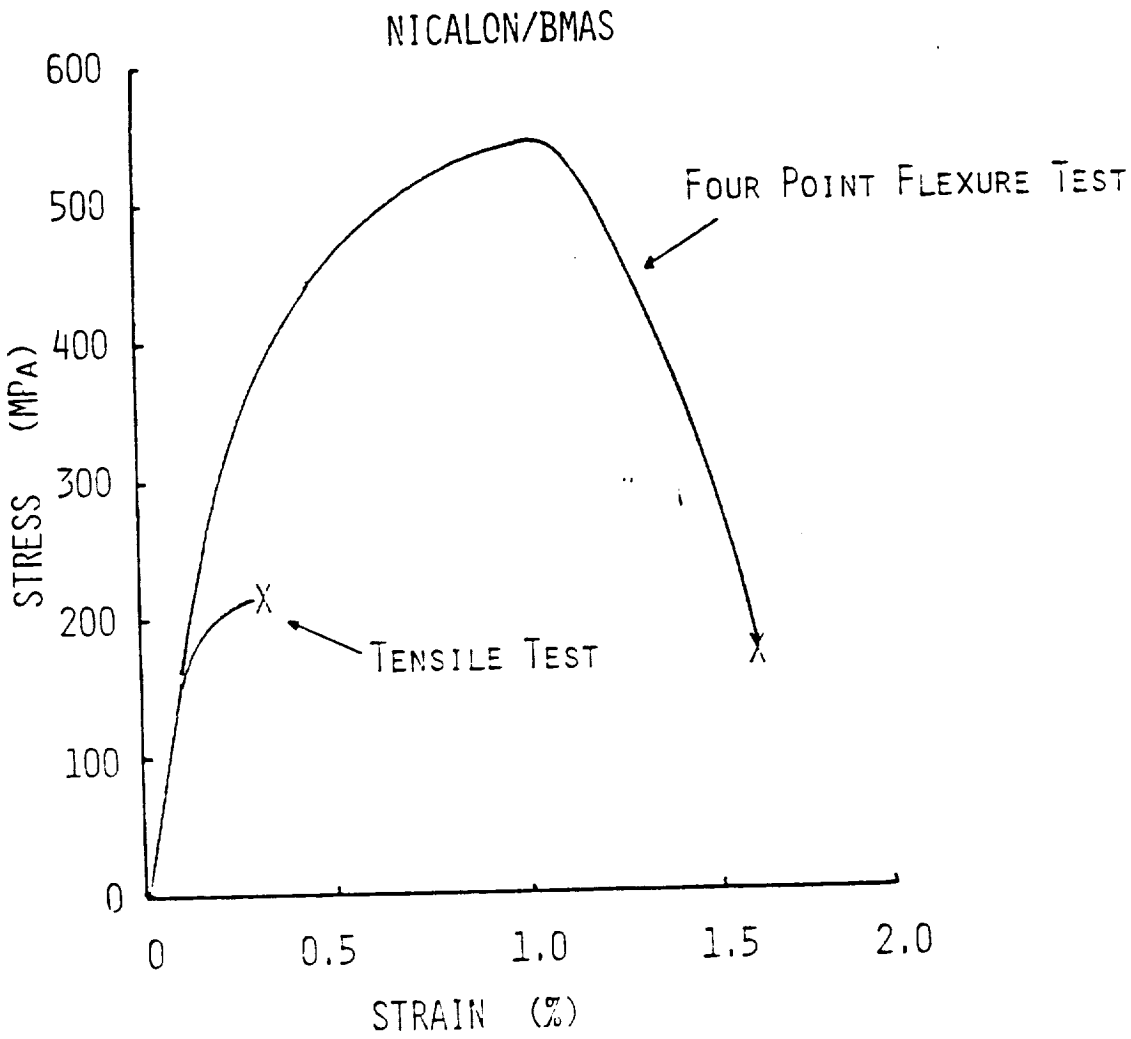

FIGURE 1 COMPARISON OF TENSILE AND FLEXURAL STRESS-STRAIN CURVES FOR LONGITUDINAL NICALON/BMAS COMPOSITE AT 20°C.

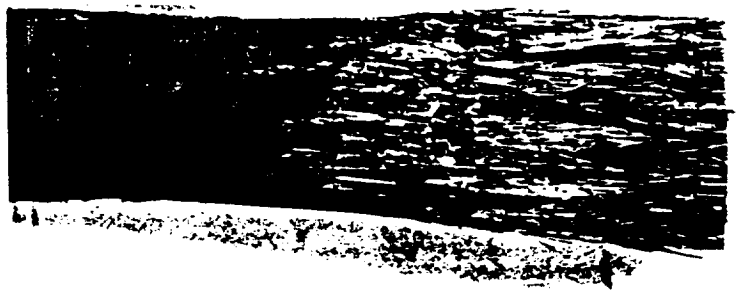

FIGURE 2

SURFACE DAMAGE FROM SERRATED GRIP FACE

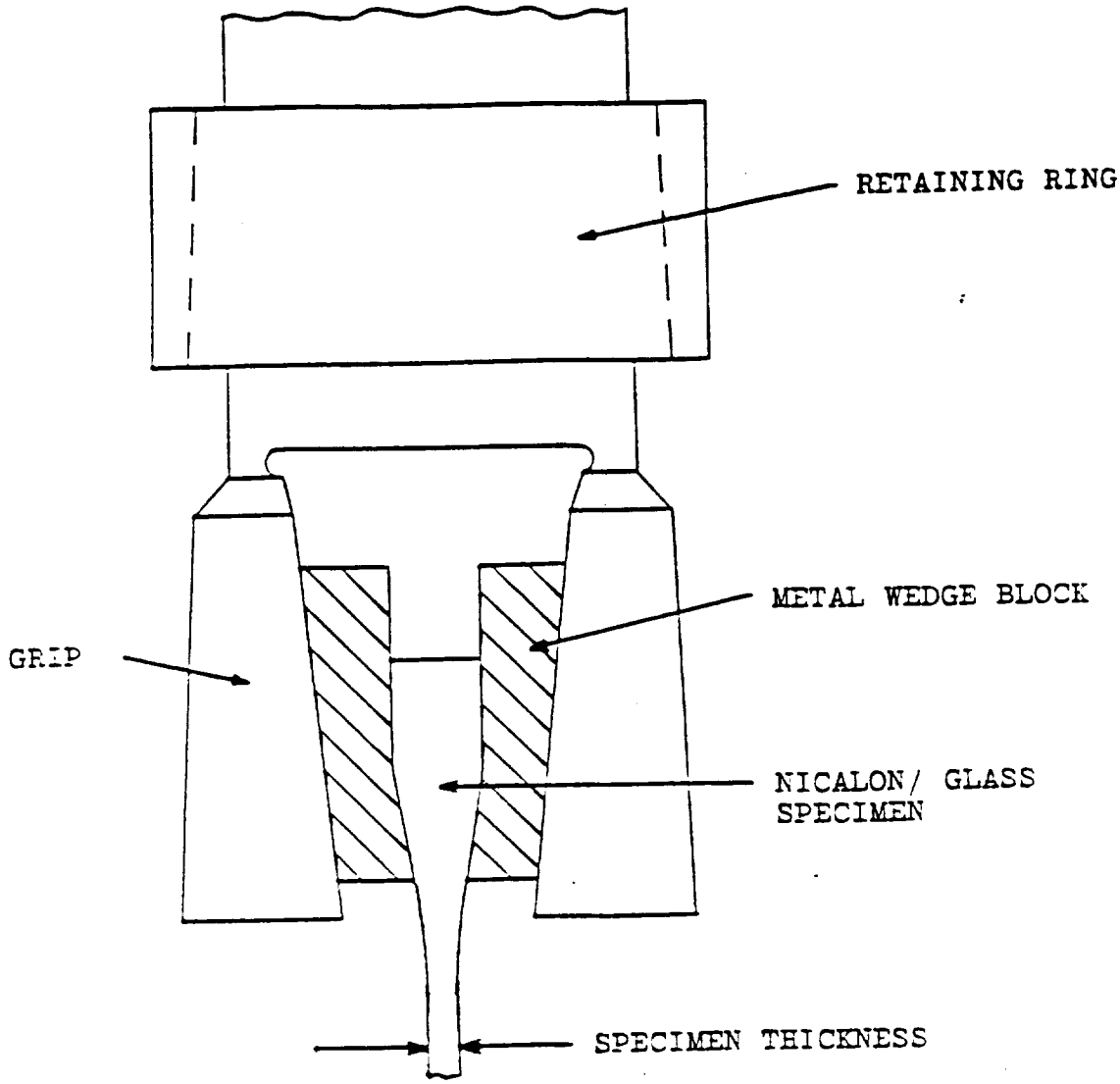

FIGURE 3 Tensile Test Specimen in Grip

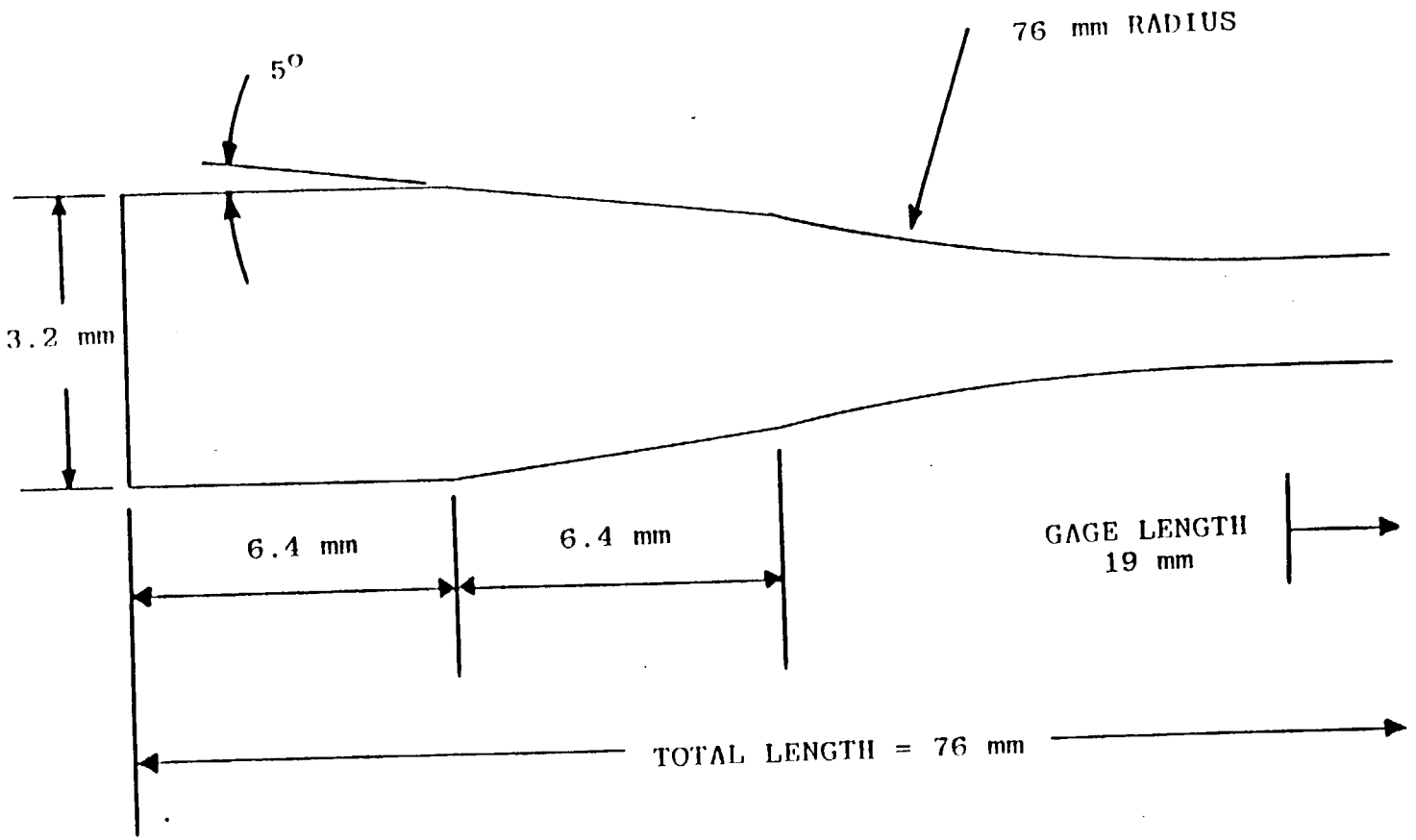

FIGURE 4 THICKNESS-TAPERED TENSILE SPECIMEN GEOMETRY

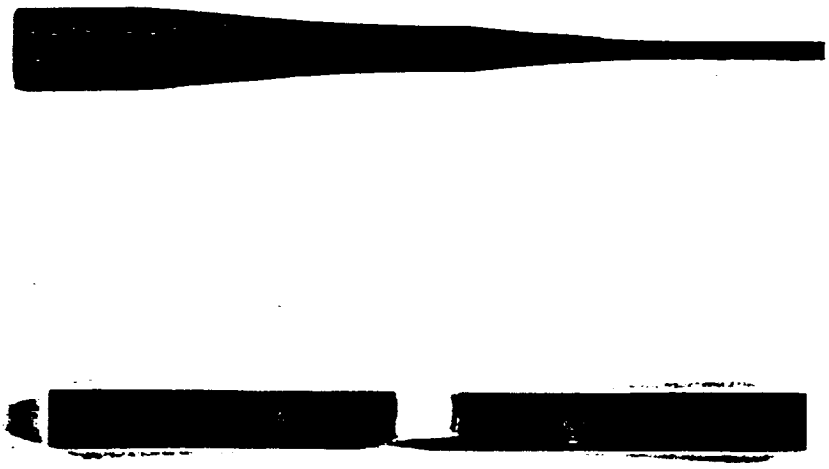

FIGURE 5 FAILED LONGITUDINAL NICALON/1723 THICKNESS-TAPERED SPECIMEN; EDGE VIEW (TOP) AND FACE VIEW.

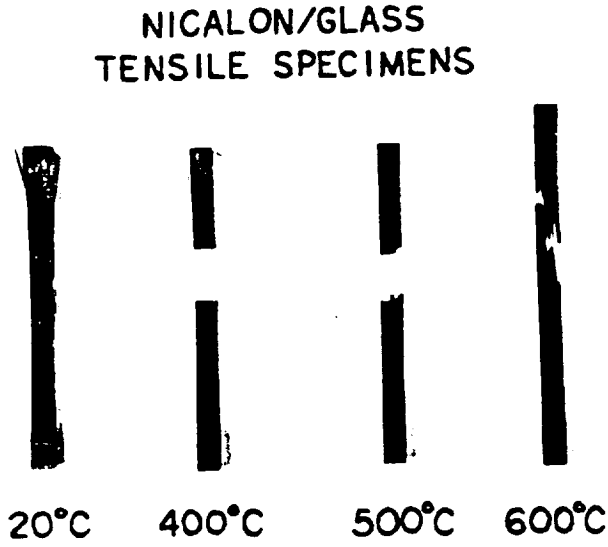

FIGURE 6

TYPICAL BROKEN SPECIMENS FROM NEW TENSILE TEST METHOD

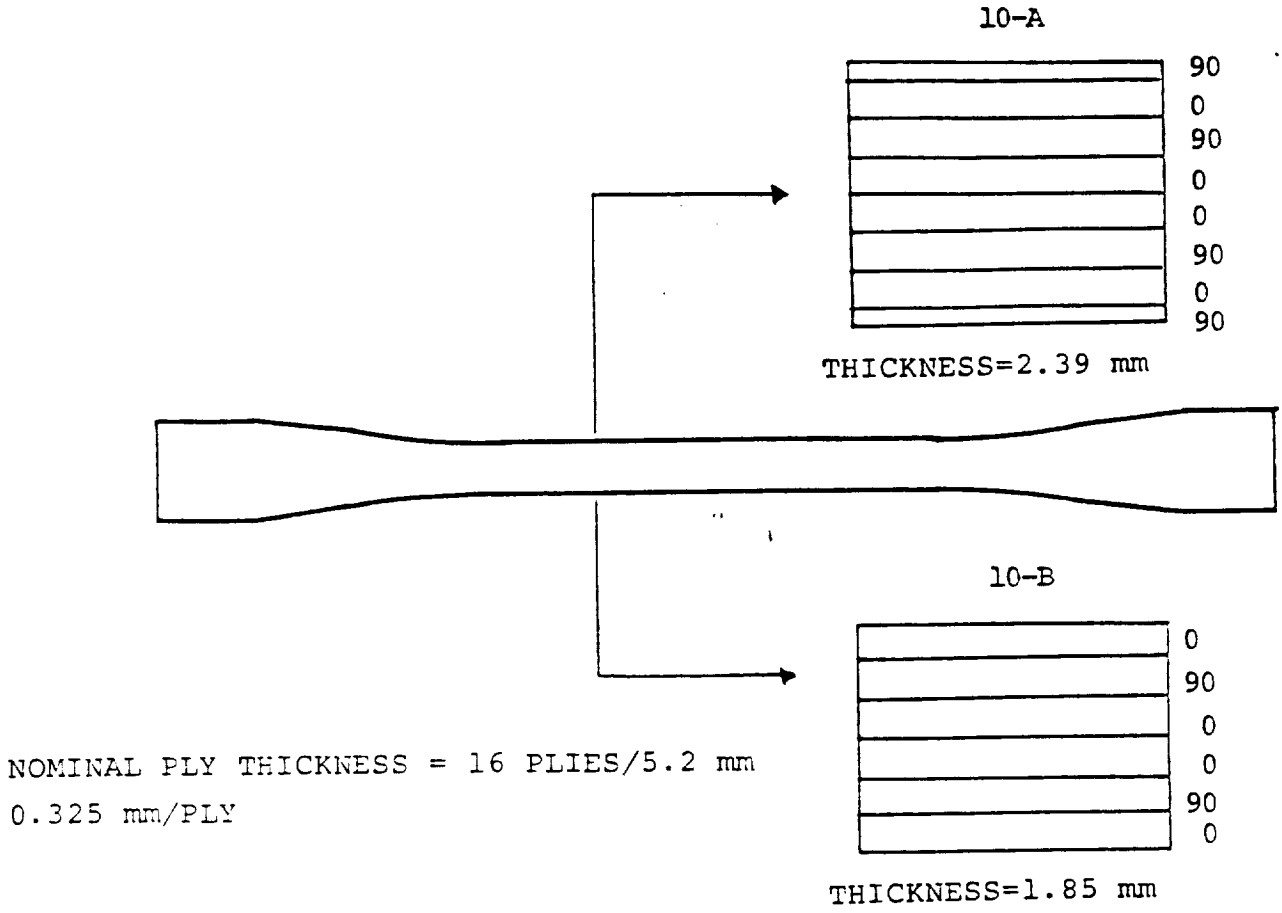

FIGURE 7 - Ply stacking sequence for specimens 10-A and 10-B.

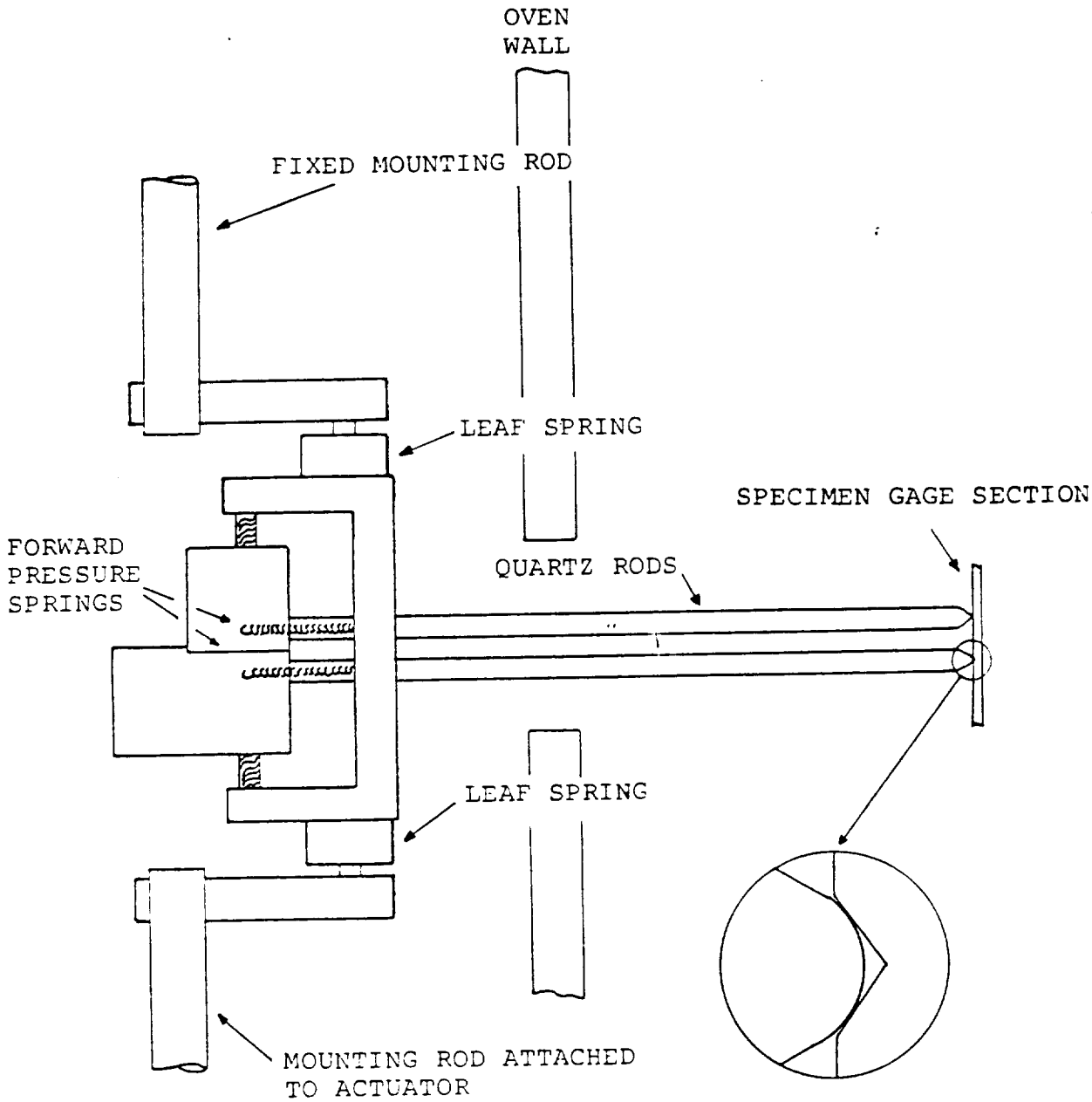

FIGURE 8 SCHEMATIC OF LONGITUDINAL EXTENSOMETER AND DETAIL OF ROD TIP AT SPECIMEN SURFACE DIVOT.

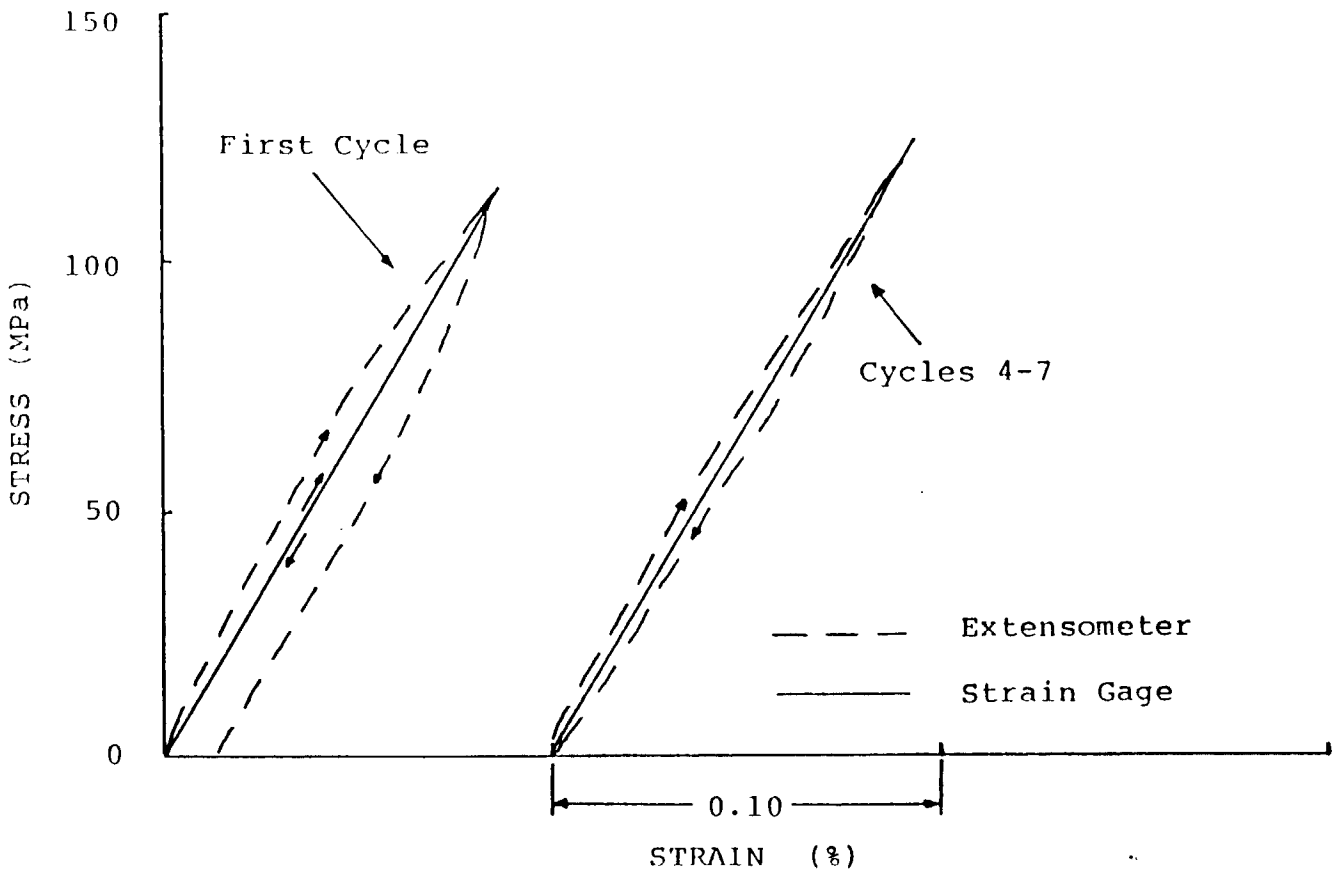

FIGURE 9 TENSILE STRESS-STRAIN RESPONSE FROM EXTENSOMETER WITH POORLY SEATED ROD TIP AS COMPARED WITH STRAIN GAGES ON THE SAME SPECIMEN, SHOWING FIRST AND SUBSEQUENT LOADING-UNLOADING CYCLES FOR LONGITUDINAL NICALON/1723 GLASS SPECIMEN.

FIGURE 10 Tensile Stress-Strain Curve (With Cycles) Longitudinal Nicalon/1723 Tested at 20°C

UNIDIRECTIONAL NICALON/ GLASS COMPOSITE.

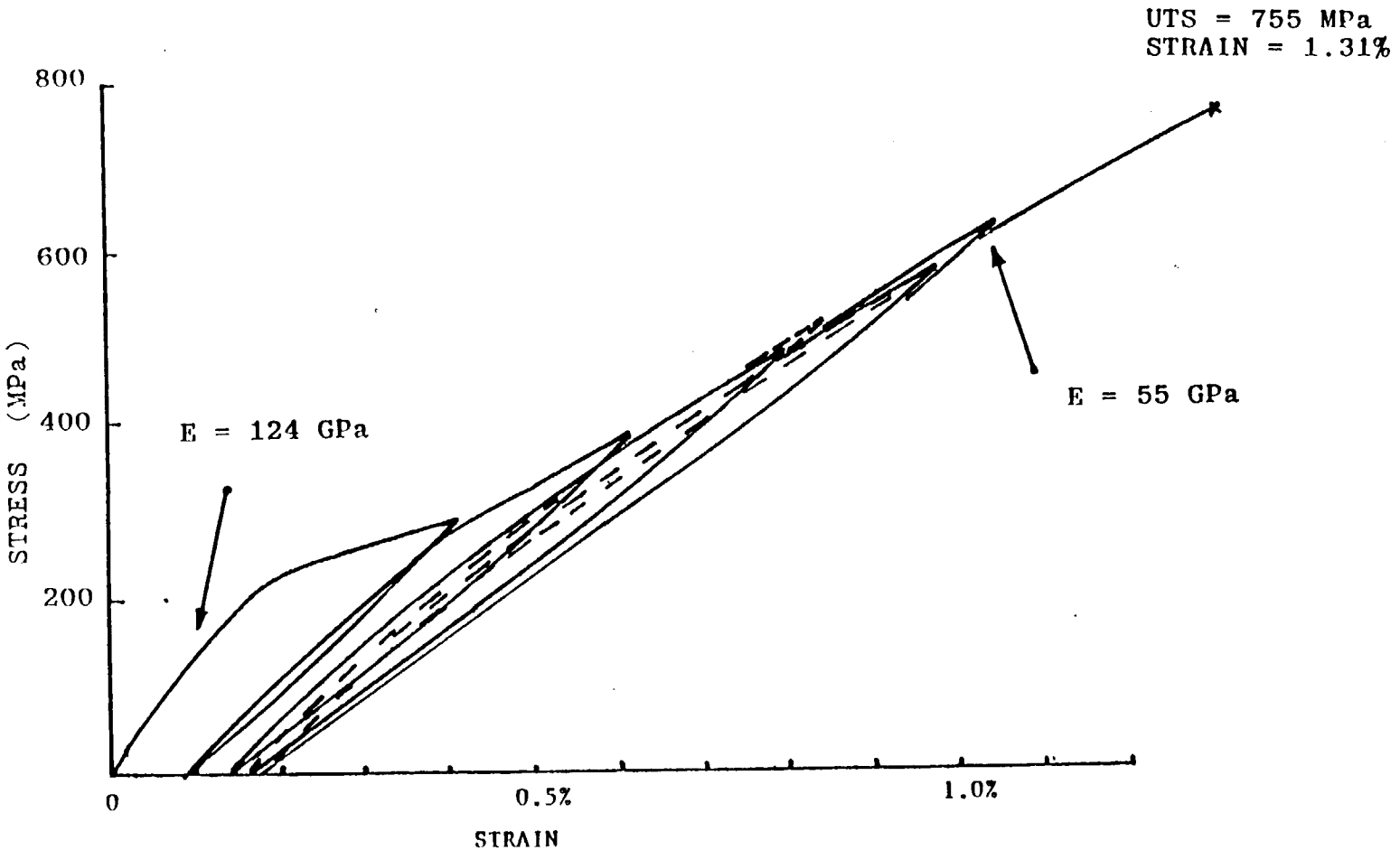

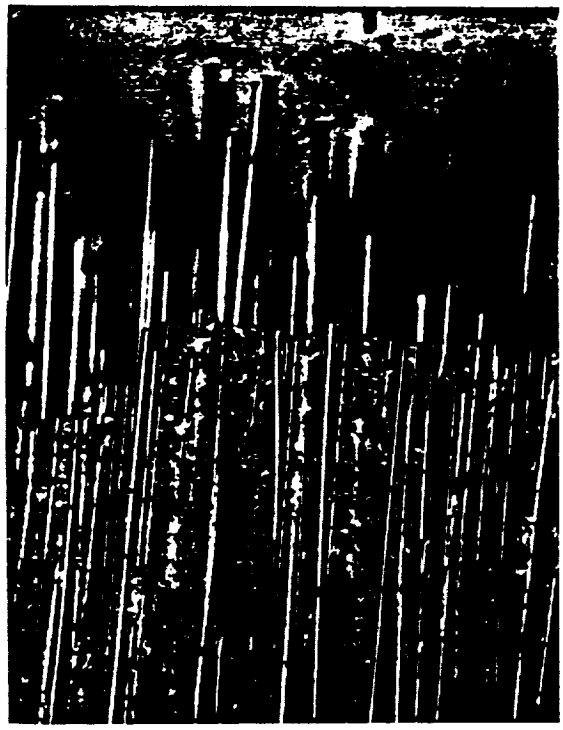

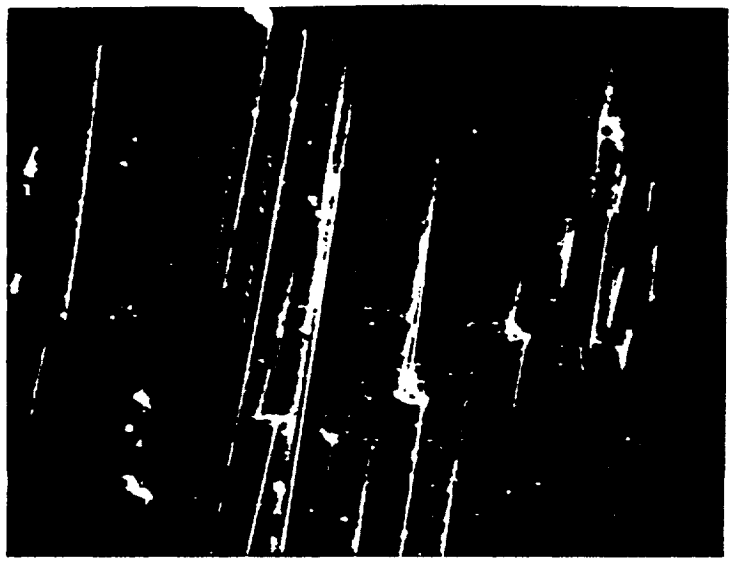

FIGURE 11 Fracture Profile and Matrix Cracking For Longitudinal Nicalon/1723 Tested at 20°C

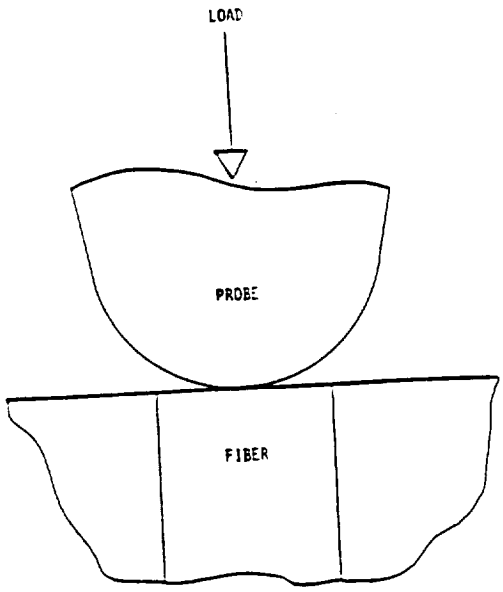

FIGURE 12 Schematic of Single Fiber Loading in Microdebonding Test Method

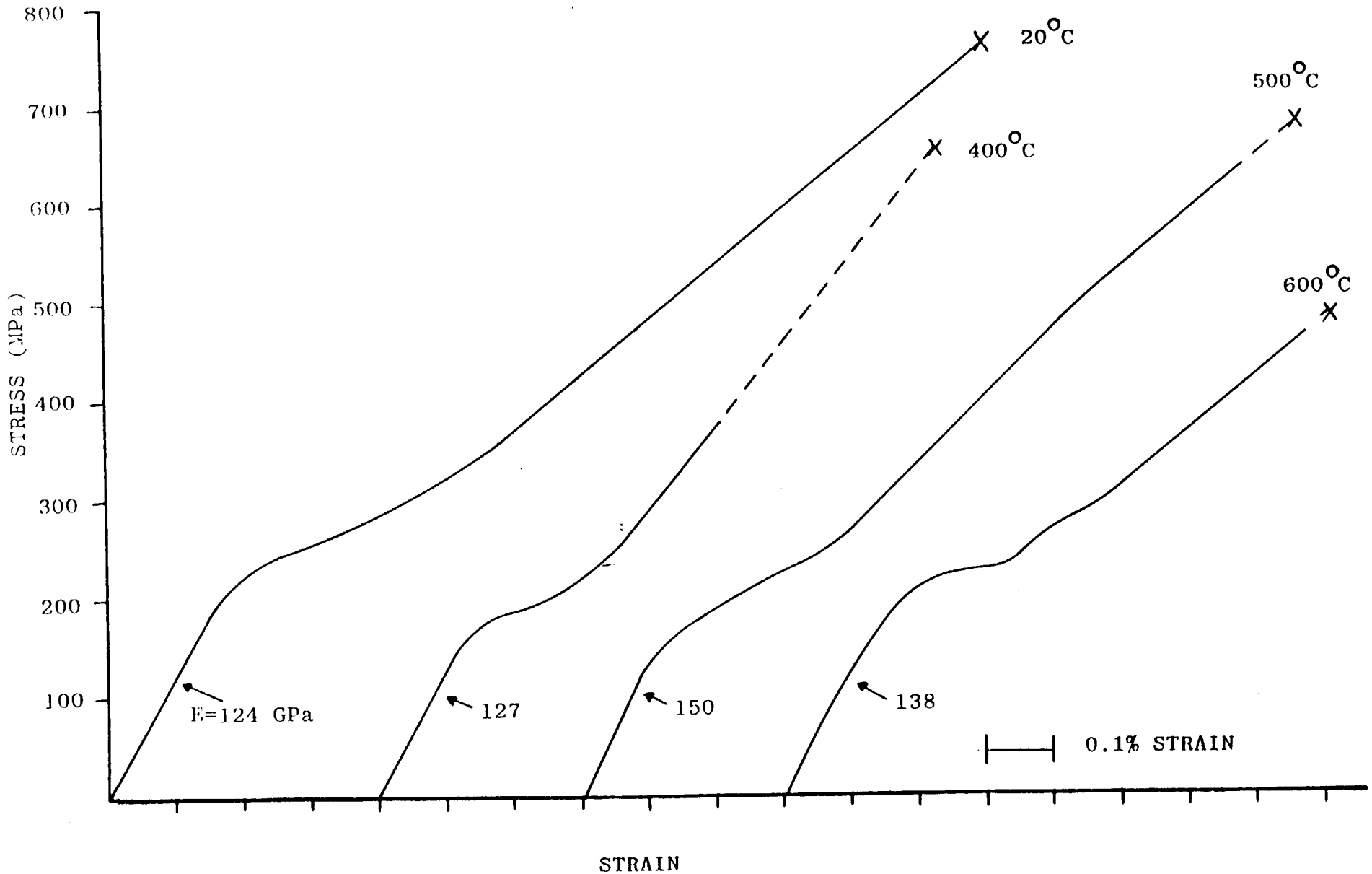

FIGURE 13 TYPICAL TENSILE STRESS-STRAIN CURVES FOR LONGITUDINAL NICALON/1723 GLASS VS. TEMPERATURE

FIGURE 14 Longitudinal Tensile Strength of Nicalon/1723 vs. Test Temperature

NICALON/ GLASS COMPOSITE.

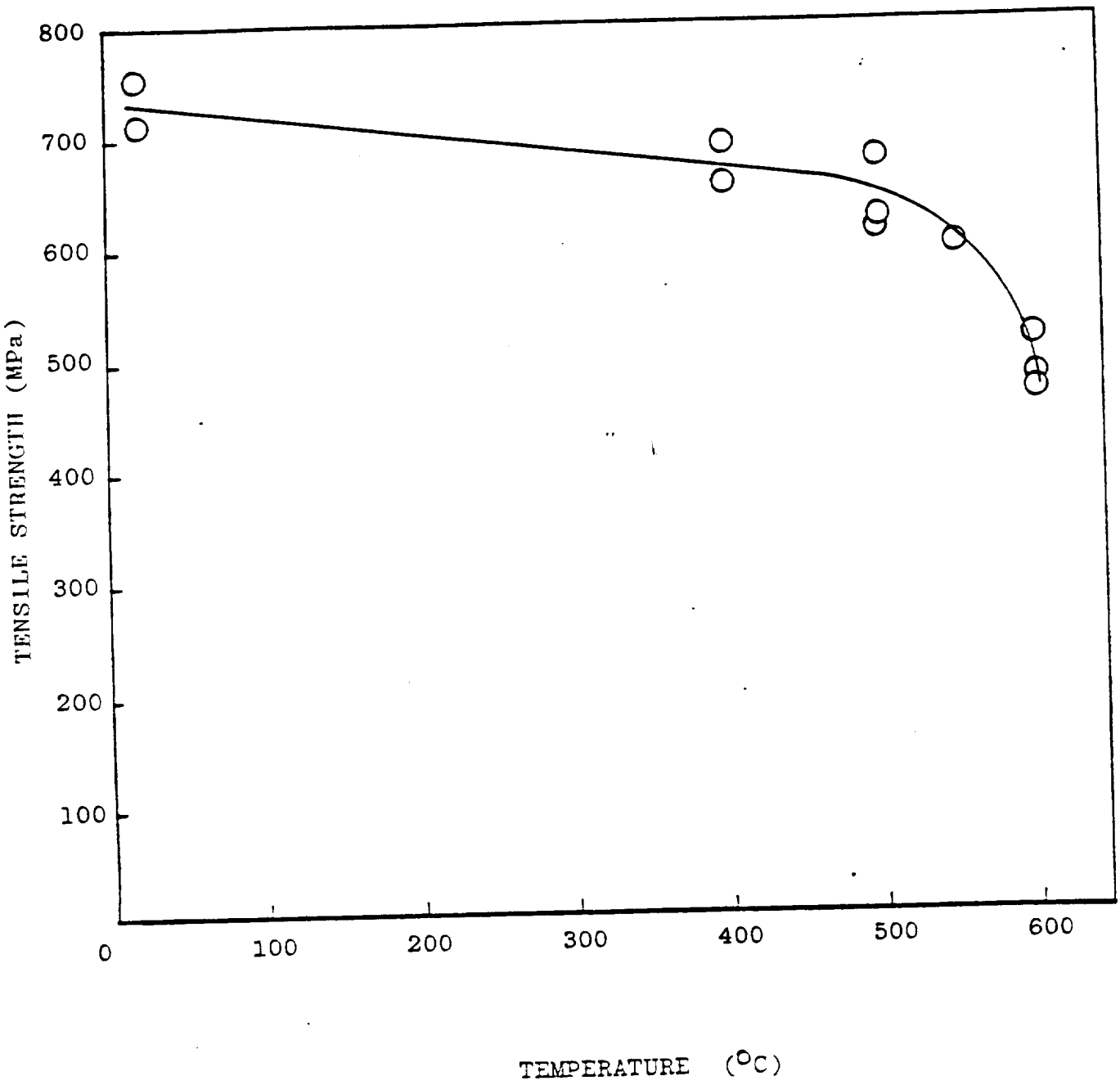

FIGURE 15

EXTENSIVE FIBER PULLOUT FOR ONE SPECIMEN AT 600°C

NICALON/1723 GLASS

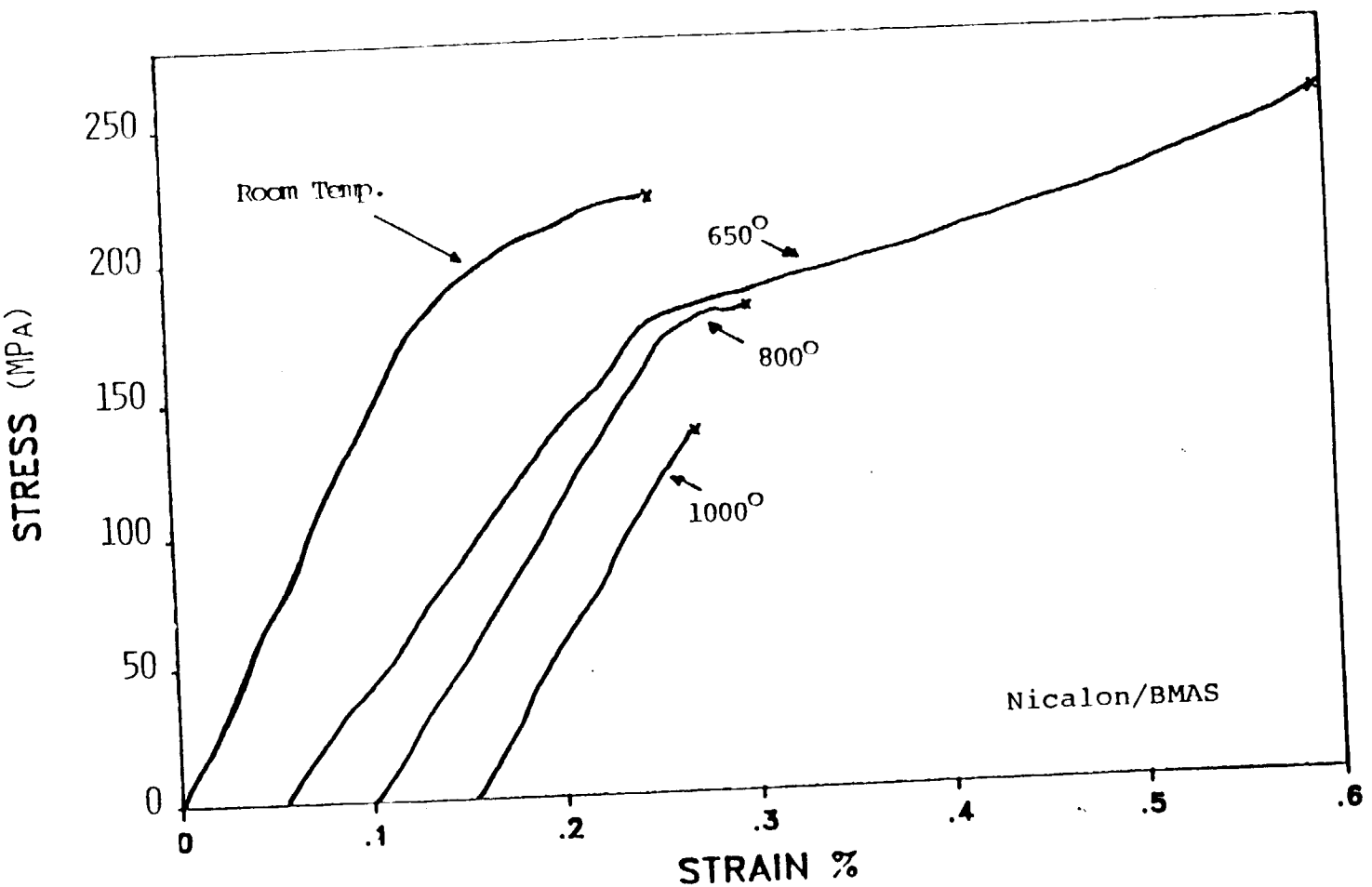

FIGURE 16 TYPICAL TENSILE STRESS-STRAIN CURVES FOR LONGITUDINAL NICALON/BMAS GLASS-CERAMIC VS. TEMPERATURE (NON-OPTIMIZED BATCH).

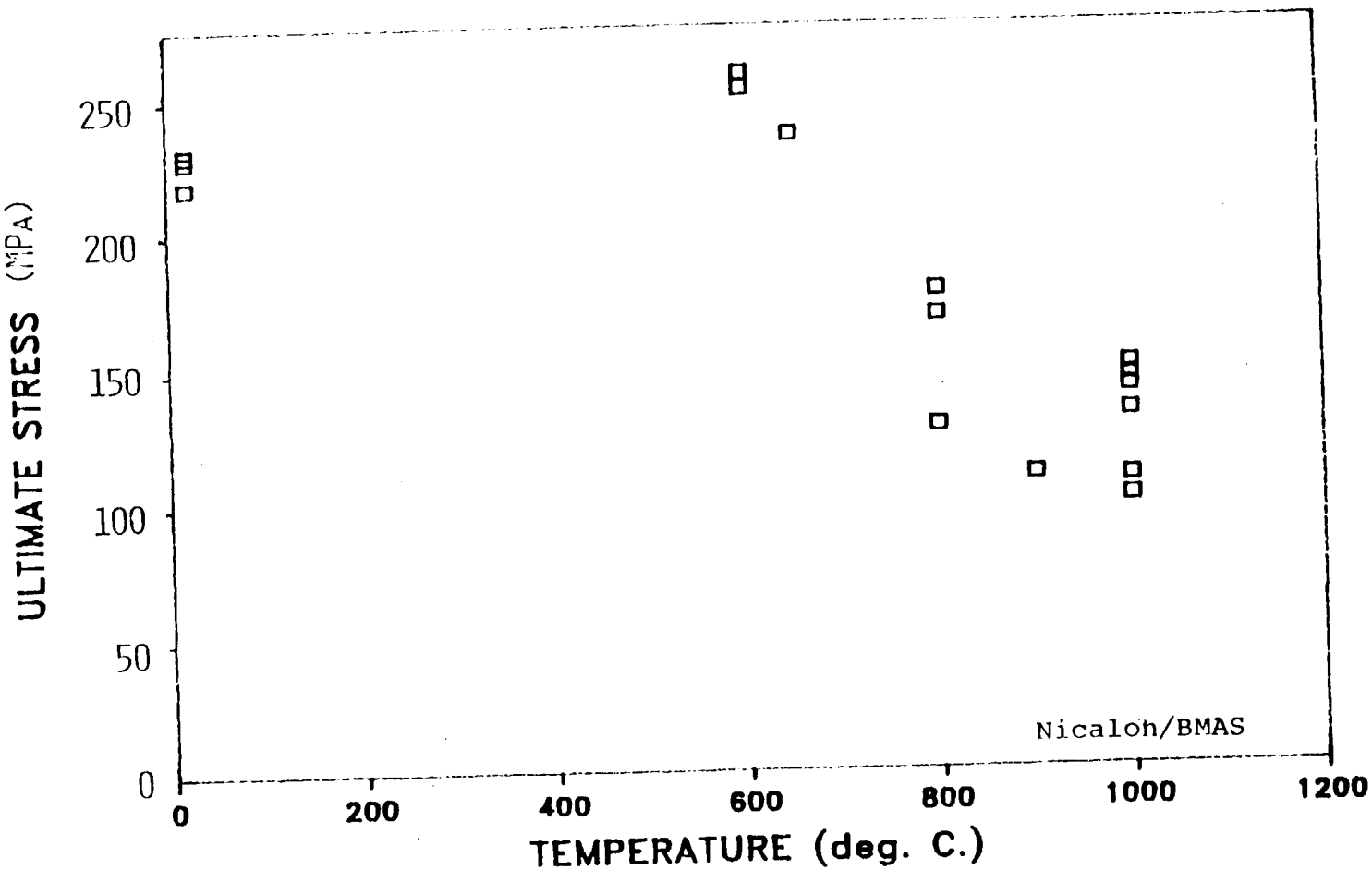

FIGURE 17 Longitudinal Tensile Strength of Nicalon/BMAS vs. Test Temperature.

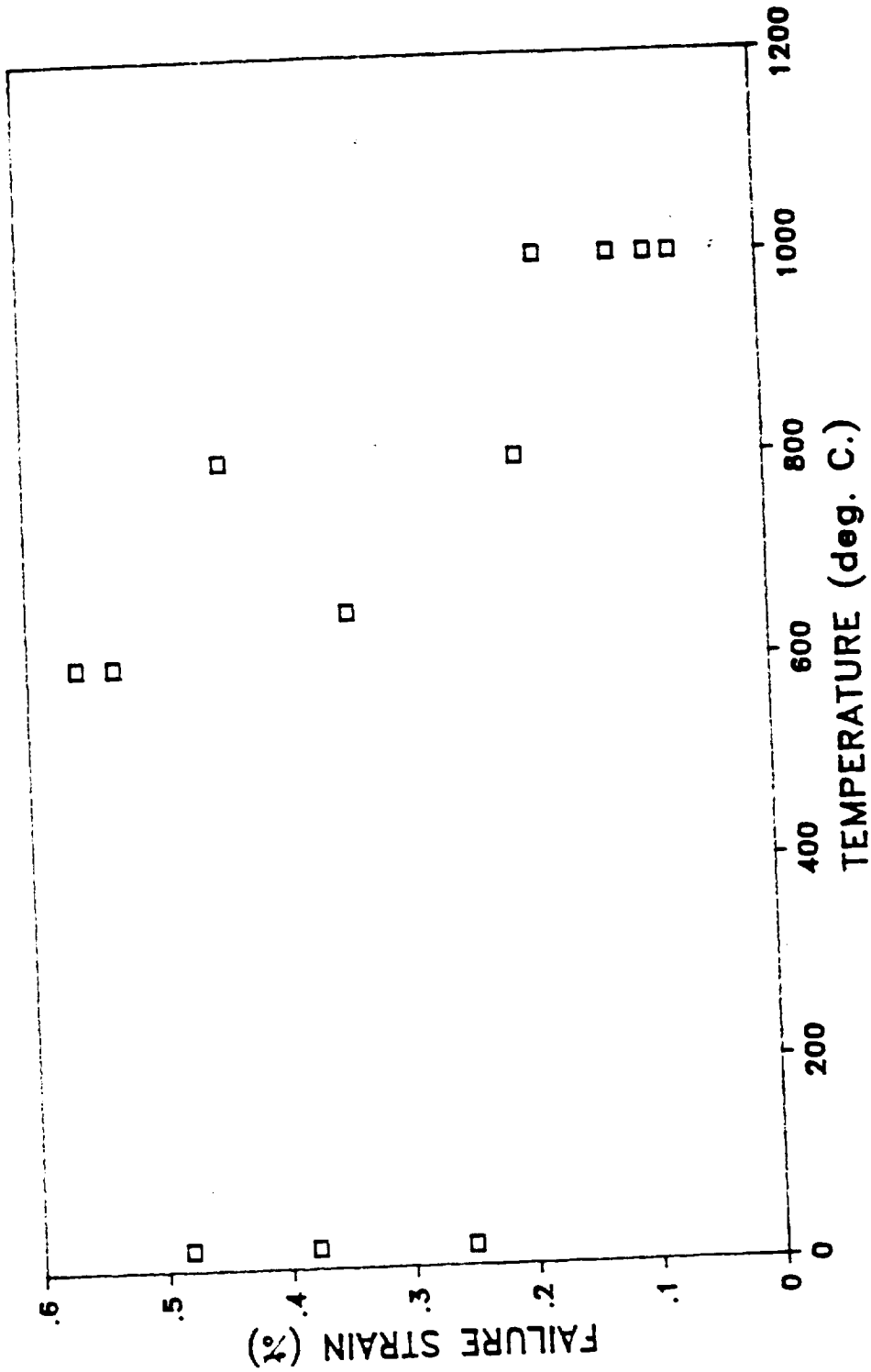

FIGURE 18 Longitudinal Failure Strain of Nicalon/BMAS vs. Test Temperature.

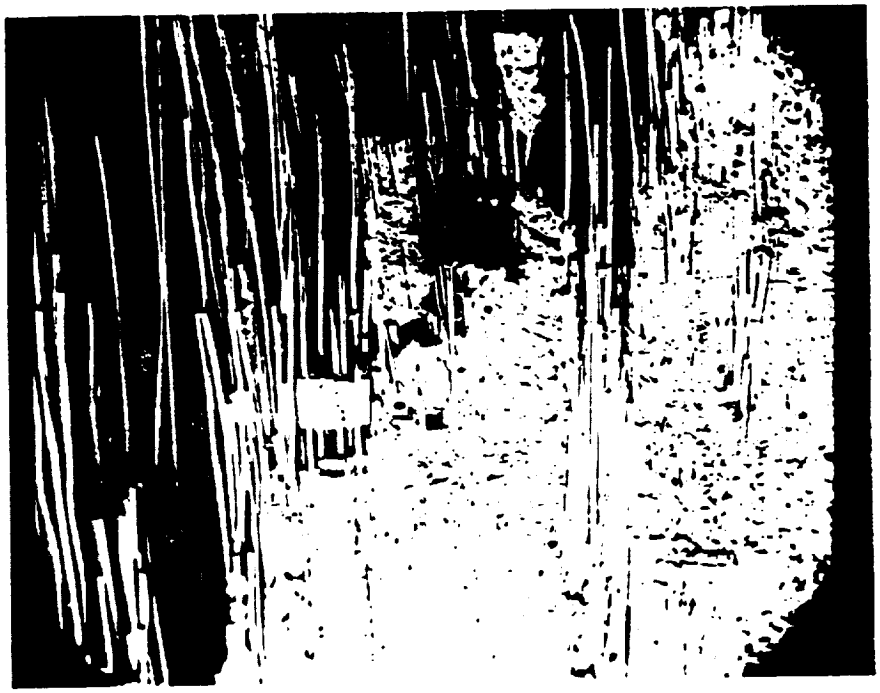

TESTED AT
23° C

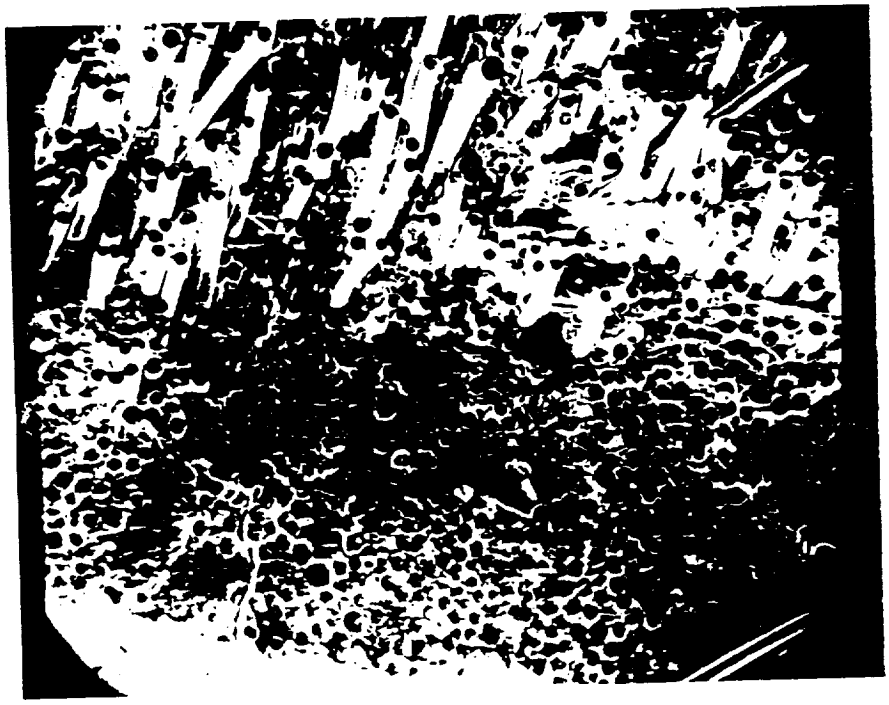

TESTED AT
1000° C

FIGURE 19 Nicalon/BMAS Tensile Failure at 20°C and 1000°C (Near Edge

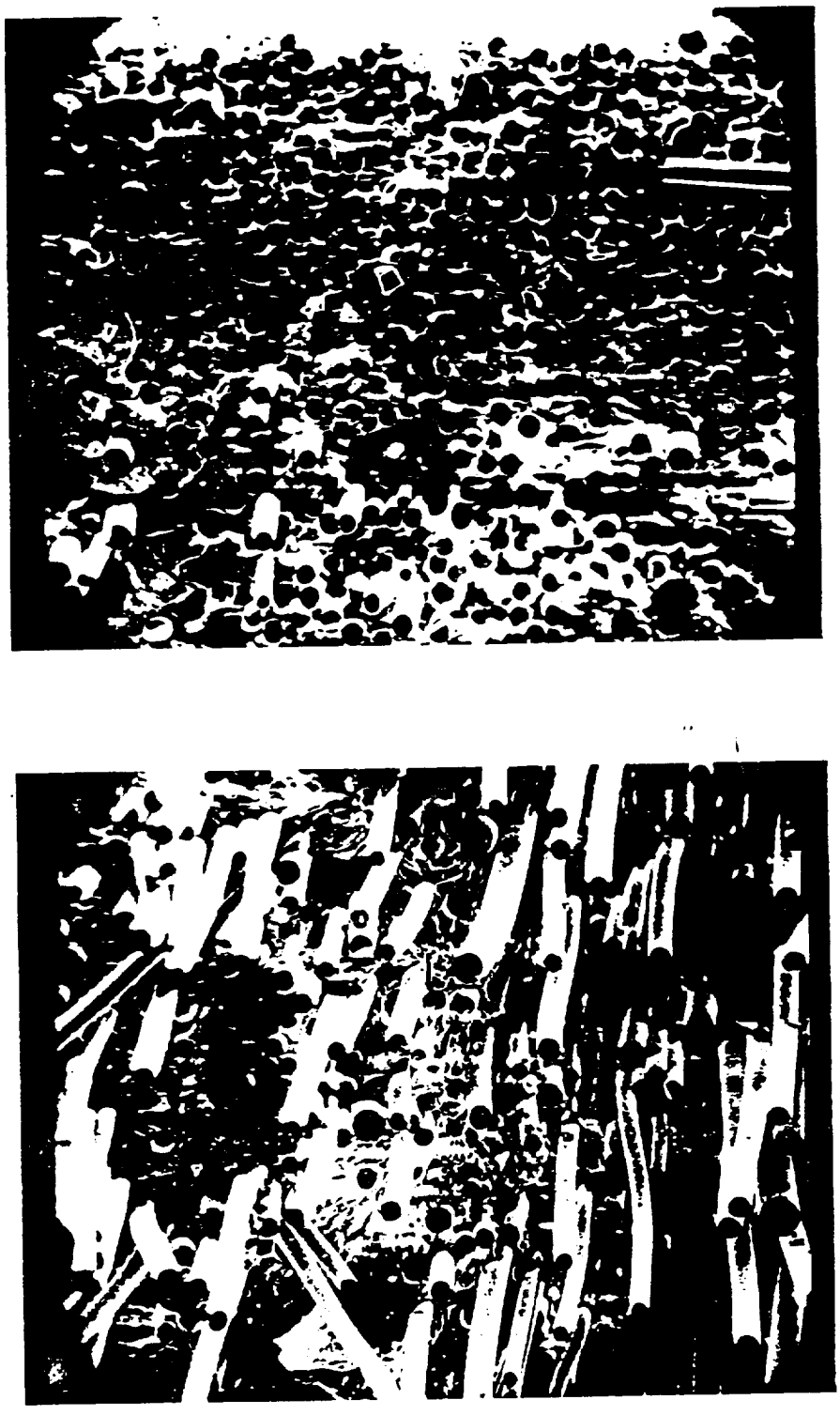

FIGURE 20 Fracture Surfaces of Nicalon/BMAS Tensile Failure Tested at 1000°C Showing Embrittled Zone at Surface and Pullout on Interior.

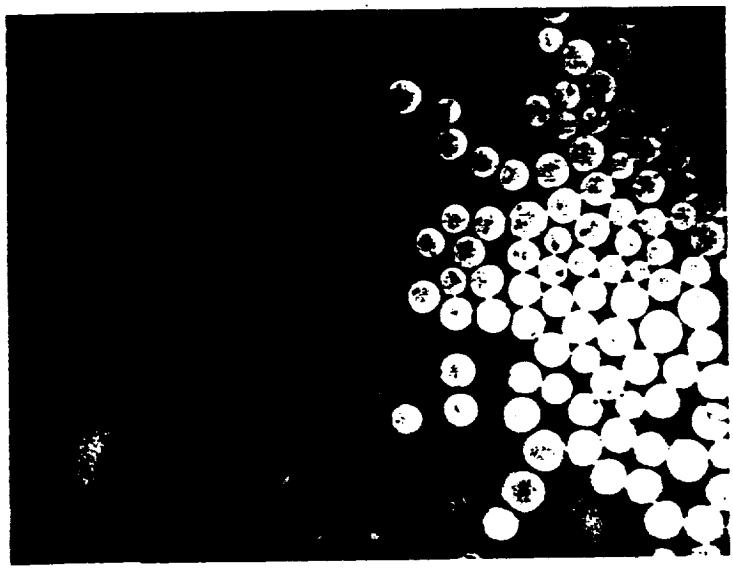

MOLDED
EDGE

EDGE

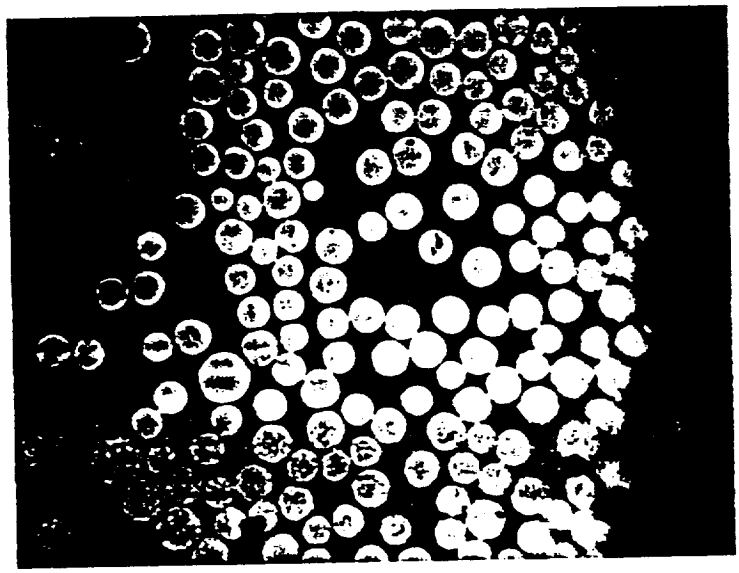

MACHINED
EDGE

FIGURE 21 Polished Cross-Section of Nicalon/BMAS Block Exposers. at 1000°C in Air, Showing the Molded and Ground Edge Regions.

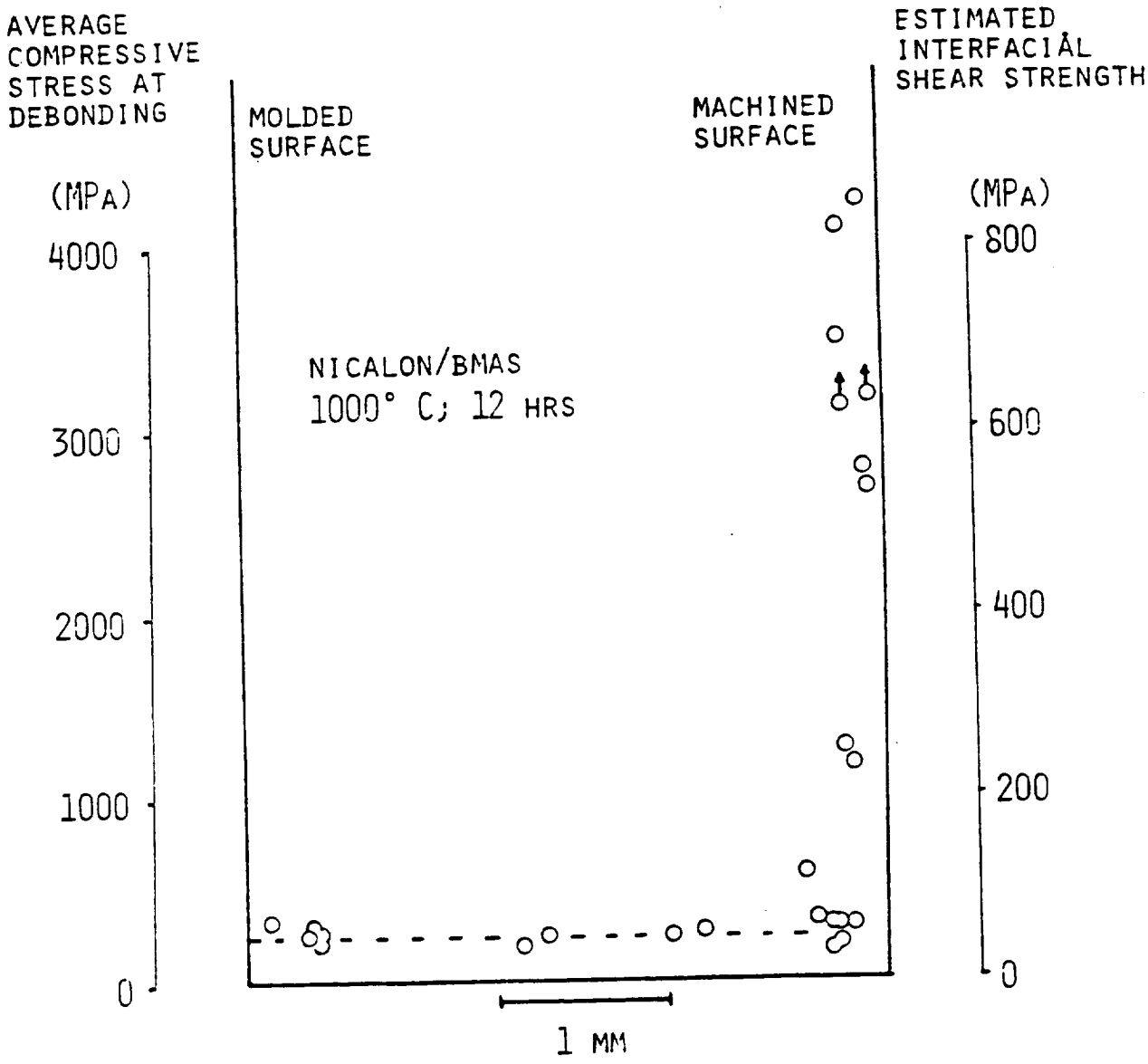

FIGURE 22 In-Situ Fiber/Matrix Interfacial Shear Strength From Microdebonding Test Plotted Across the Cross-Section in Figure 12.

FIGURE 23 FRONT AND BACK STRAIN GAGE RESPONSE FOR 0/90 NICALON/BMAS SPECIMEN NO. 10B AT 20°C.

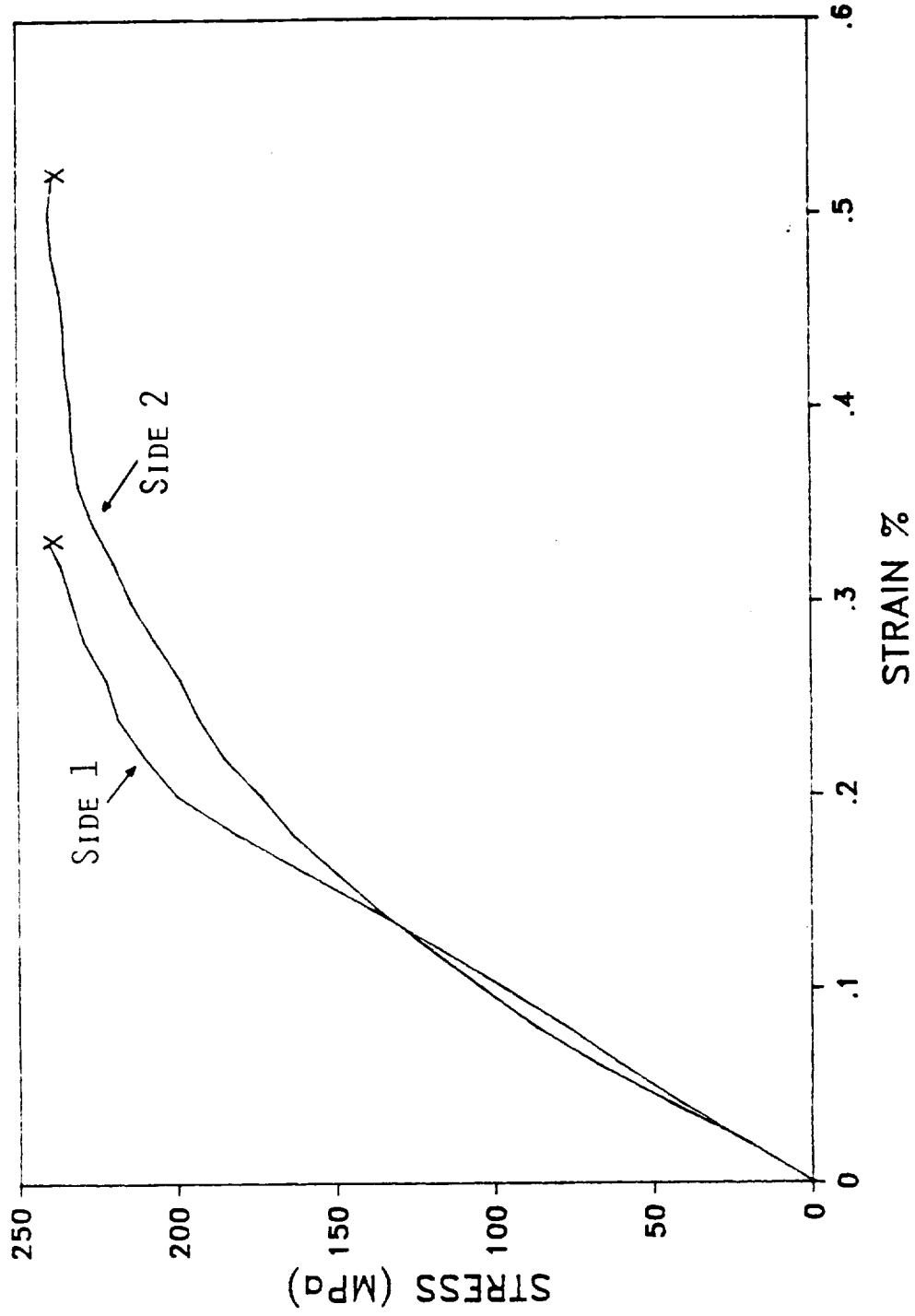

PAGE _____ INTENTIONALLY BLANK

REPORT DOCUMENTATION PAGE

Form Approved
OMB No. 0704-0188

1. AGENCY USE ONLY (Leave blank)	2. REPORT DATE	3. REPORT TYPE AND DATES COVERED
	October 1991	Final Contractor Report

4. TITLE AND SUBTITLE
Structural Characterization of High Temperature Composites

5. FUNDING NUMBERS
WU-505-63-5B

6. AUTHOR(S)
J.F. Mandell and D.H. Grande

7. PERFORMING ORGANIZATION NAME(S) AND ADDRESS(ES)
Massachusetts Institute of Technology
Department of Materials Science and Engineering
Cambridge, Massachusetts 02139

8. PERFORMING ORGANIZATION REPORT NUMBER
None

9. SPONSORING/MONITORING AGENCY NAMES(S) AND ADDRESS(ES)
National Aeronautics and Space Administration
Lewis Research Center
Cleveland, Ohio 44135-3191

10. SPONSORING/MONITORING AGENCY REPORT NUMBER
NASA CR-187220

11. SUPPLEMENTARY NOTES
Project Manager, C.C. Chamis, Structures Division, NASA Lewis Research Center, (216) 433-3252.

12a. DISTRIBUTION/AVAILABILITY STATEMENT
Unclassified - Unlimited
Subject Category 24

12b. DISTRIBUTION CODE

13. ABSTRACT *(Maximum 200 words)*

Glass, ceramic, and carbon matrix composite materials have emerged in recent years with potential properties and temperature resistance which make them attractive for high temperature applications such as gas turbine engines. At the outset of this study, only flexural tests were available to evaluate brittle matrix composites at temperatures in the 600 to 1000 °C range. This report describes the results of an ongoing effort to develop appropriate tensile, compression and shear test methods for high temperature use. A tensile test for unidirectional composites has been developed and used to evaluate the properties and behavior of ceramic fiber reinforced glass and glass-ceramic matrix composites in air at temperatures up to 1000 °C. The results indicate generally efficient fiber reinforcement and tolerance to matrix cracking similar to polymer matrix composites. Limiting properties in these materials may be an inherently very low transverse strain to failure, and high temperature embrittlement due to fiber/matrix interface oxidation.

14. SUBJECT TERMS	15. NUMBER OF PAGES
Ceramic; Glass matrix; Nicalon fiber; Tension shear; Temperature; Interface oxidation	58
	16. PRICE CODE: A04

17. SECURITY CLASSIFICATION OF REPORT	18. SECURITY CLASSIFICATION OF THIS PAGE	19. SECURITY CLASSIFICATION OF ABSTRACT	20. LIMITATION OF ABSTRACT
Unclassified	Unclassified	Unclassified	

NASA